Discovery of N-Hydroxyindole-Based Inhibitors of Human Lactate Dehydrogenase Isoform A (LDH-A) as Starvation Agents against Cancer Cells

ARTICLE *in* JOURNAL OF MEDICINAL CHEMISTRY · FEBRUARY 2011

Impact Factor: 5.45 · DOI: 10.1021/jm101007q · Source: PubMed

Journal of Medicinal Chemistry

ARTICLE

pubs.acs.org/jmc

Discovery of *N*-Hydroxyindole-Based Inhibitors of Human Lactate Dehydrogenase Isoform A (LDH-A) as Starvation Agents against Cancer Cells

Carlotta Granchi,[†] Sarabindu Roy,[†] Chiara Giacomelli,[†] Marco Macchia,[†] Tiziano Tuccinardi,[†] Adriano Martinelli,[†] Mario Lanza,[‡] Laura Betti,[‡] Gino Giannaccini,[‡] Antonio Lucacchini,[‡] Nicola Funel,[§] Leticia G. León,[∥,⊥] Elisa Giovannetti,[⊥] Godefridus J. Peters,[⊥] Rahul Palchaudhuri,[#] Emilia C. Calvaresi,[#] Paul J. Hergenrother,[#] and Filippo Minutolo*[,†]

[†]Dipartimento di Scienze Farmaceutiche and [‡]Dipartimento di Psichiatria, Neurobiologia, Farmacologia, e Biotecnologie, Università di Pisa, Via Bonanno 6, 56126 Pisa, Italy

[§]Dipartimento di Chirurgia (Anatomia Patologica), Università di Pisa, Via Roma 57, 56126 Pisa, Italy

[∥]Institudo Universitario de Bio-Organica "Antonio Gonzales", Universidad de La Laguna, Avda. Astrofisico F. Sánchez 2, La Laguna, 38206-Tenerife, Spain

[⊥]Department of Medical Oncology, VU University Medical Center, De Boelelaan 1117, 1081 HV Amsterdam, The Netherlands

[#]Department of Chemistry, University of Illinois, 600 S. Mathews Avenue, Urbana, Illinois 61801, United States

Supporting Information

ABSTRACT: Highly invasive tumor cells are characterized by a metabolic switch, known as the Warburg effect, from "normal" oxidative phosphorylation to increased glycolysis even under sufficiently oxygenated conditions. This dependence on glycolysis also confers a growth advantage to cells present in hypoxic regions of the tumor. One of the key enzymes involved in glycolysis, the muscle isoform of lactate dehydrogenase (LDH-A), is overexpressed by metastatic cancer cells and is linked to the vitality of tumors in hypoxia. This enzyme may be considered as a potential target for new anticancer agents, since its inhibition cuts cancer energetic and anabolic supply, thus reducing the metastatic and invasive potential of cancer cells. We have discovered new and efficient *N*-hydroxyindole-based inhibitors of LDH-A, which are isoform-selective (over LDH-B) and competitive with both the substrate (pyruvate) and the cofactor (NADH). The antiproliferative activity of these compounds was confirmed on a series of cancer cell lines, and they proved to be particularly effective under hypoxic conditions. Moreover, NMR experiments showed that these compounds are able to reduce the glucose-to-lactate conversion inside the cell.

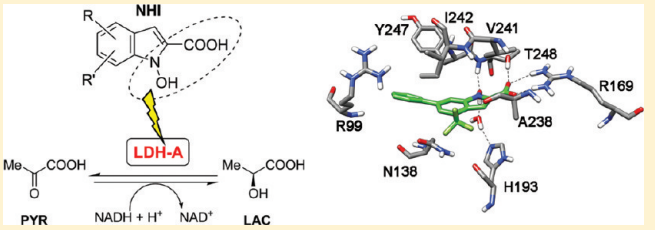

INTRODUCTION

Unlike normal cells, most invasive tumor phenotypes show a metabolic switch, named the "Warburg effect",[1] from oxidative phosphorylation to an increased rate of glycolysis. This switch ensures a sufficient energy supply from glucose and thus high vitality, even in hypoxic environments.[2,3] This unusual metabolic trait is particularly advantageous in solid tumors, which are generally significantly less oxygenated than normal tissues. Once their dimension reaches certain values (usually >1 cm^3), solid tumors present hypoxic regions surrounding necrotic areas. Hypoxic cancers pose a great challenge to oncologists all over the world because they are especially aggressive, metastatic, and resistant to (1) radiotherapy, mainly because of scarce formation of oxygen-dependent cytotoxic radicals upon irradiation, and (2) chemotherapy because of limited blood supply and also because they have a slow rate of proliferation, whereas most of the currently available therapies target rapidly dividing cells. Moreover, hypoxia increases the cancer stem cell fraction and promotes acquisition of a stemlike state, thus increasing chances of cancer relapse.[4] This metabolic situation is accompanied by (1) higher consumption of glucose, due to the lower efficiency in energy production by glycolysis (Figure 1), and (2) increased extracellular acidosis because of the high production of lactic acid and other acidic species. It may be possible, however, to take advantage of this peculiar metabolic feature of cancer cells for selective anticancer therapy.[5]

There are only a few molecules in preclinincal studies or clinical trials that are known to exploit, or interfere with, the increased glycolytic process of invasive tumors.[6,7] Lonidamine,

Received: August 4, 2010

   dx.doi.org/10.1021/jm101007q | *J. Med. Chem.* XXXX, XXX, 000–000

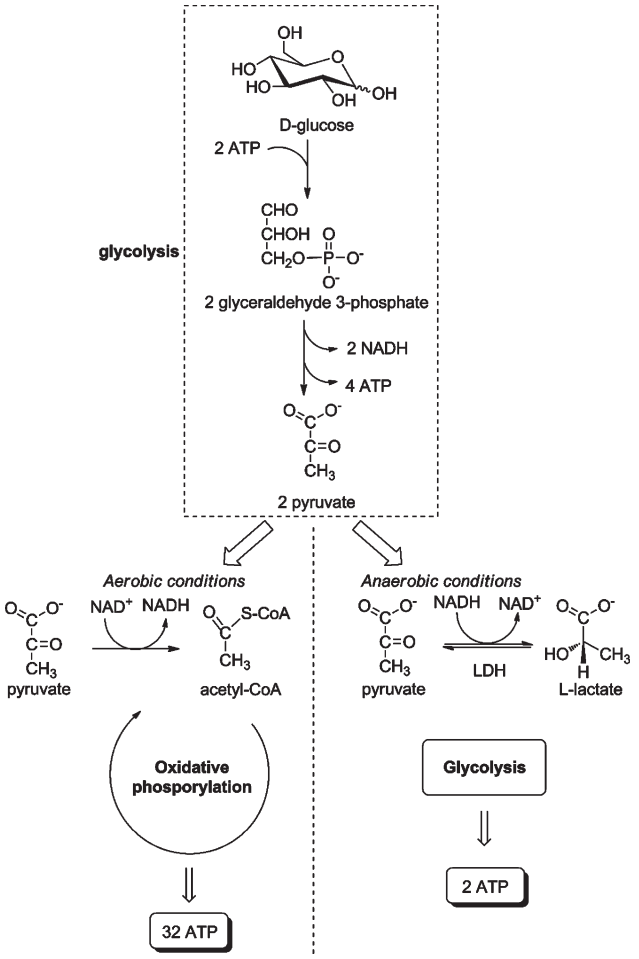

Figure 1. Fate of pyruvate during glycolysis under aerobic and anaerobic conditions: role of LDH.

an inhibitor of hexokinase (HK), the enzyme that catalyzes the phosphorylation of the 6-position of glucose, thus starting the glycolytic process, has completed a phase 3 trial, but its efficacy was undermined by pancreatic and hepatic toxicity.[8] Among HK inhibitors, 2-deoxyglucose (2-DG) showed promising results in a phase 1 trial, but its action on hypoxic tumors was not satisfactory,[9] and 3-bromopyruvate induces apoptosis in some carcinomas, but no clinical tests are yet available.[10] Dichloroacetate (DCA) is a pyruvate dehydrogenase kinase (PDK) inhibitor under phase 1 clinical study whose action restores the normal oxidative demolition of pyruvate by reactivating pyruvate dehydrogenase (PDH) and thus indirectly diverting glycolysis,[11] although some concerns stem from recent evidence that PDK-knockout has no effect on the proliferation and survival of hypoxic tumor cells.[12] Increased glucose uptake occurring in invasive tumors was clinically exploited by a prodrug, glufosfamide, which has completed clinical trials on several tumors and is composed of an alkylating moiety linked to a β-D-glucose unit that takes advantage of the transmembrane glucose transport system, which is greatly increased in malignant phenotypes.[13] Finally, the suitability of the fetal isoform of pyruvate kinase (PK-M2), overexpressed by invasive tumors,[14] as a potential target for the development of isoform-specific inhibitors[15] is currently under debate because its inhibition may lead to paradoxical effects on cancer growth.[16] Indeed, a recent report describes the development of PK-M2 activators based on a diarylsulfonamide scaffold, which were intended as prospective antiproliferative agents.[17]

Lactate dehydrogenase (LDH) constitutes a major checkpoint for the switch from aerobic to anaerobic glycolysis by catalyzing the reduction of pyruvate into lactate (Figure 1). In humans, LDH is a tetrameric enzyme that may exist in five isoforms (*h*LDH1−5), mostly located in the cytosol. There are only two types of subunits: LDH-A (or LDH-M, muscle) and LDH-B (or LDH-H, heart). The five isoforms are made up of the various possible combinations of these two subunits in the following way: LDH1 = LDH-B_4, LDH2 = LDH-AB_3, LDH3 = LDH-A_2B_2, LDH4 = LDH-A_3B, LDH5 = LDH-A_4. *h*LDH1 is mostly represented in the heart, whereas *h*LDH5 is prevalent in liver and skeletal muscle. *h*LDH5 has been found to be overexpressed in highly invasive and hypoxic carcinomas, and it was clearly associated with hypoxia inducible factor HIF-1α.[18] Serum and plasma *h*LDH5 levels are used as tumor biomarkers, and these levels are not necessarily correlated to nonspecific cellular damage. Rather they are caused by overexpression induced by malignant tumor phenotypes.[19] An amplified expression of this gene, measured as LDH-A subunit increased production, was found in several tumor lines.[20] This, together with the overexpression of glucose transporter GLUT1 due to oxygen deprivation,[20] further promotes glycolysis. Furthermore, lactate production contributes to extracellular acidosis, thus supporting tumor invasivity and exerting an immunosuppressive effect.[21]

LDH-A (for the sake of clarity, from now on we will refer to this monomeric subunit also for the fully functional tetrameric *h*LDH5) was recently acknowledged as one of the most promising tumor targets.[22] In fact, repression of its expression by shRNA cuts the main energy production sequence in hypoxic tumors, as shown by a reduced invasiveness in metastatic cell lines. More recently, subclones of the breast cancer cell line MDA-MB-435 that were resistant to paclitaxel were shown to be resensitized upon either down-regulation of LDH-A by siRNA or after chemical inhibition of LDH-A activity by oxamate.[23] Furthermore, inhibition of LDH-A is unlikely to give rise to major side effects in humans, since hereditary LDH-A deficiency causes myoglobinuria only after intense anaerobic exercise, whereas it does not provoke any symptoms under ordinary circumstances.[24] Therefore, compounds able to inhibit LDH-A enzymatic activity may constitute safe agents able to interfere with tumor growth and invasiveness on many fronts. For these reasons, we have decided to pursue "druglike" small molecules able to inhibit *h*LDH5.

Few LDH inhibitors are reported in the literature, and most of them were developed against the isoform present in *P. falciparum* (*pf*LDH), as this enzyme was conceived as a valid target for the treatment of malaria. The inhibitory activity of these compounds against human LDH isoforms was reported as a possible side effect, and in many cases the inhibition levels were extremely low.[25] Oxamate (OXM, Figure 2), still considered as the LDH-A reference inhibitor, is competitive with the pyruvate substrate, but it is nonselective and not very potent, with a K_i of 138 μM (vs pyruvate).[26] Another known LDH-A inhibitor is gossypol, a natural polyphenol dialdehyde extracted from cotton seeds, which is also highly cytotoxic and promiscuous.[27] Some very small azoles possessing vicinal OH and COOH groups, such as 3-hydroxyisoxazole-4-carboxylic acid (HICA, Figure 2) and 4-hydroxy-1,2,5-thiadiazole-3-carboxylic acid (HTCA, Figure 2) showed IC_{50} values of 54 and 10 μM, respectively, on LDH-A, and the hydroxyl−carboxylic substitution pattern proved to be

dx.doi.org/10.1021/jm101007q |*J. Med. Chem.* XXXX, XXX, 000–000

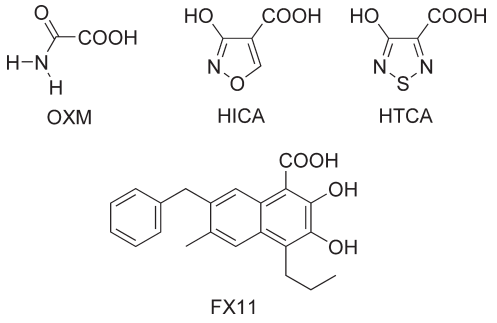

Figure 2. Structures of some of the most significant LDH-A inhibitors.

essential for their inhibitory activity. Unfortunately, these compounds have such simple structures that their selective action is not guaranteed. Thiadiazole derivative HTCA cannot be functionalized further, and any substituent placed in the only free position of isoxazole HICA has afforded inactive compounds.[28] Thus, these azoles are not ideal candidates for further optimization. Finally, derivatives of 8-deoxyhemigossylic (2,3-dihydroxynaphtalen-1-carboxylic) acid, originally designed as antimalarial agents,[29] have furnished some of the most effective and selective LDH-A inhibitors. One of these compounds, FX11 (Figure 2), is a LDH-A inhibitor competitive with the reduced nicotinamide adenine dinucleotide (NADH) cofactor, displaying a K_i of 8 μM on LDH-A and a >10-fold selectivity over the other isoform LDH-B, which was very recently shown to inhibit tumor progression by inducing an oxidative stress to the cancer cells.[30] Although FX11 contains a potentially redox-active catechol moiety that may make it unsuitable as a drug, it is an important proof-of-concept for LDH-A inhibition as a tractable anticancer strategy.

The X-ray crystal structure of the LDH-A subunit of *h*LDH5[31] shows that the active site is located in a rather deep position within the protein and accessibility to it is narrow. This cavity normally hosts both the substrate (pyruvate) and the cofactor (NADH). Overall, it is quite polar and rich in cationic residues (arginines). This would explain why the inhibitors so far discovered (Figure 2) have carboxylates, closely associated with a hydroxyl or a carbonyl oxygen atom. This information is consistent with the natural LDH substrates, an α-hydroxy acid (lactate) or an α-keto acid (pyruvate), that are thus mimicked by the inhibitors. We have considered these pharmacophore requirements and the first of a series of hydroxycarboxylates positioned on various aromatic scaffolds never explored before in this field, such as an unusual class of heterocyclic derivatives, the *N*-hydroxyindoles (NHI),[32] bearing a carboxylic acid group in the 2-position (Chart 1). The NHI scaffold has been largely neglected in the design of biorelevant molecules, possibly because of the relative lack of synthetic methods for its assembly. On the contrary, numerous isolated natural products have been discovered to contain NHI portions, such as nocathiacin I, a stable antibiotic,[33] and the most significant NHI preparations are essentially represented by a reduction of the indole system to 2,3-dihydroindole, followed by an oxidation step (Na_2WO_4/H_2O_2) or by a $SnCl_2$-promoted reduction of carbonyl-substituted nitroarenes.[34,35]

Compounds **1a**−**k** were thus designed to retain the hydroxyl−carboxylate motifs of other LDH-A inhibitors (Figure 2), with the difference that their N−OH group is slightly less acidic than typical phenol groups.[36] A series of exploratory simple substitution patterns (halogens, phenyl, trifluoromethyl, and tetrazole) were selected to determine if it was possible

Chart 1. *N*-Hydroxyindoles (NHI) Designed as LDH-A Inhibitors (1a−k)

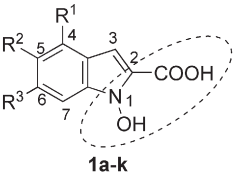

1a-k

compound	R^1	R^2	R^3
1a	H	H	H
1b	CH_3	H	H
1c	CF_3	H	H
1d	Cl	H	H
1e	Br	H	H
1f	H	H	Br
1g	C_6H_5	H	H
1h	H	C_6H_5	H
1i	H	H	C_6H_5
1j	CF_3	H	C_6H_5
1k	H	H	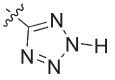

to achieve satisfactory levels of LDH-A inhibition within this chemical class.

RESULTS AND DISCUSSION

Synthetic Chemistry. The synthetic pathway generally followed for the preparation of NHI **1a**−**k** is shown in Scheme 1. The first step involved a reaction of nitrotoluenes **2a**−**k** with sodium hydride and an excess of dimethyl oxalate in DMF at −15 °C to room temperature. These conditions worked nicely for all the nitrotoluene derivatives with the exception of **2j**, which was instead treated with potassium *tert*-butoxide in diethyl ether and the minimum amount of methanol needed to dissolve the substrate. In this manner the condensation of the resulting anion with dimethyl oxalate efficiently afforded ketoester **3j**. The resulting α-ketoesters **3a**−**j** were then treated with $SnCl_2 \cdot 2H_2O$ in DME at 0 °C in the presence of 4 Å molecular sieves.[35] In most cases, these conditions promoted the desired reductive cyclization to build the NHI scaffold, whereas in two cases (**3h,i**) mixtures with the over-reduced indole (**9h,i**, Scheme 2) derivatives were obtained, and in one case (tetrazole **3k**) only a complex mixture of products was produced. In this latter case, we changed the condition to a combination of sodium hypophosphite and catalytic palladium over charcoal[37] and successfully obtained the tetrazole-substituted NHI **4k**. Subsequent hydrolysis with aqueous 2 N LiOH in a THF/MeOH mixture afforded the final products **1a**−**k**. Noncommercially available precursors **2j** and **2k** were respectively prepared by a Pd-catalyzed cross-coupling of 5-iodo-2-methyl-3-nitrobenzotrifluoride **5**[38] with phenylboronic acid under ligand-free conditions in a microwave reactor[39] and by a zinc-promoted addition of sodium azide[40] to benzonitrile **6**. An example of *O*-methylated NHI (**8**) was also synthesized to verify the importance of the free OH group in the enzyme inhibition assays. For this purpose, NHI **4i** was treated with iodomethane and DBU in THF at room temperature to give ester **7**, which was eventually hydrolyzed to compound **8**.

As mentioned, during the reductive cyclization step of phenyl-substituted ketoesters **3h,i** to NHI **4h,i**, we actually obtained

dx.doi.org/10.1021/jm101007q |*J. Med. Chem.* XXXX, XXX, 000–000

Scheme 1. Generic Synthesis of NHI 1a−k and Specific Steps for the Preparation of Precursors 2j,k and *O*-Methylated NHI 8[a]

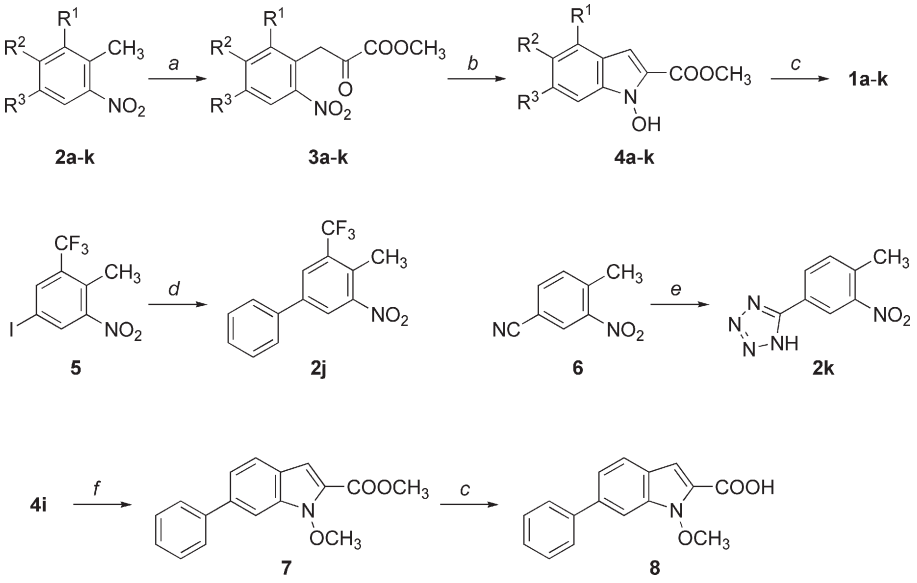

[a] Reagents and conditions. (a) For **2a−i** and **2k**: $(COOMe)_2$, NaH, DMF, −15 °C to room temp [48−87%]. For **2j**: $(COOMe)_2$, ^{t}BuOK/Et_2O−MeOH (10:1), 0 °C to room temp [82%]. (b) For **3a−j**: $SnCl_2 \cdot 2H_2O$, DME, 0 °C, 4 Å molecular sieves [21−72%]. For **3k**: $H_2PO_2Na \cdot H_2O$, Pd−C, H_2O/THF (1:1), room temp [48%]. (c) Aqueous 2 N LiOH, THF/MeOH (1:1), room temp [79−99%]; (d) $C_6H_5B(OH)_2$, $Pd(OAc)_2$, Na_2CO_3, TBAB, H_2O, 150 °C, 5 min, microwave [96%]; (e) NaN_3, $ZnBr_2$, H_2O, Δ, 36 h [90%]; (f) CH_3I, DBU, THF, room temp, 15 min [79%].

Scheme 2. Product Mixtures Deriving from $SnCl_2$-Promoted Reductive Cyclizations of α-Ketoesters 3h,i and Final Synthesis of Indole-2-carboxylates 10h,i[a]

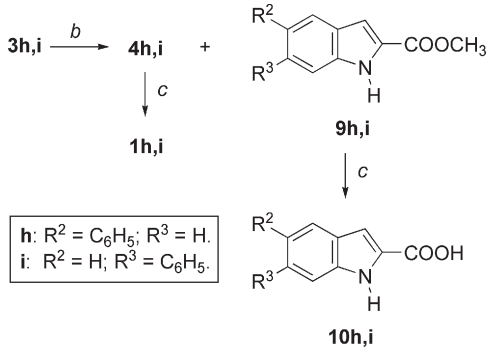

[a] Reagents and conditions: (b) $SnCl_2 \cdot 2H_2O$, DME, 0 °C, 4 Å molecular sieves [54−68% overall]; (c) aqueous 2 N LiOH, THF/MeOH (1:1), room temp [88−99%].

predominant amounts of indoles **9h,i** (the product ratios were 40:60 for **4h**/**9h** and 34:66 for **4i**/**9i**) from an over-reduction of the nitro group (Scheme 2). We separated NHI **4h,i** from **9h,i**, respectively, by column chromatography and isolated (after hydrolysis) the indolecarboxylic derivatives **10h,i**, in addition to the desired NHI **1h,i**. We considered these indole side products as valuable tools to establish the pharmacophoric portions needed for LDH-A inhibition.

Enzyme Inhibition. We started an exploratory study by assaying NHI **1a−k**, together with methyl ester **4i**, *O*-methylated NHI **8**, and indoles **10h,i**. The LDH inhibitory activities of the new compounds were measured by standard enzyme kinetic experiments on human LDH-A (as LDH5 or LDH-A_4) and LDH-B (as LDH1 or LDH-B_4) purified isoforms. Initially, we verified the percent inhibition relative to control at 125 μM for all

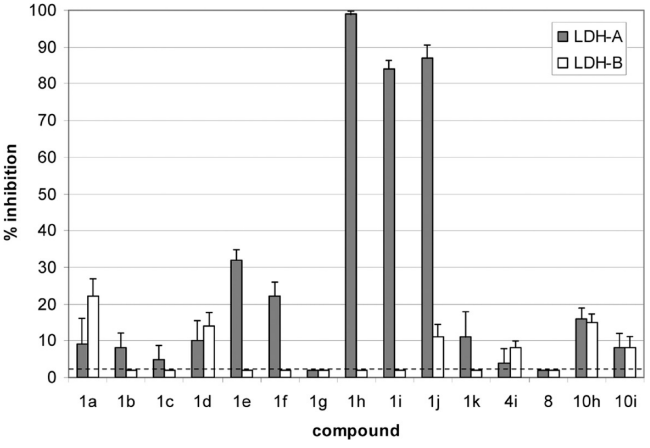

Figure 3. Colorimetric measurement of inhibition (% relative to control) of the enzymatic activity of LDH-A (gray bars) and LDH-B (white bars) in the presence of 125 μM NHI **1a−k**, ester **4i**, *O*-Me-NHI **8**, and indoles **10h,i**. Values are reported as the mean ± the SD of two or more independent experiments. Dotted line indicates the detection lower limit (3% enzyme inhibition) of this preliminary screening.

compounds with isoforms LDH-A and LDH-B (Figure 3). Briefly, the enzyme was dissolved at 37 °C in a 0.1 M phosphate buffer solution at pH 7 in the presence of the cofactor (NADH), the substrate (pyruvate), and the candidate inhibitors. Enzyme activity was determined by the measurement of the absorbance decrease at 340 nm, because of the consumption of NADH, and the percentage inhibition relative to control was plotted in Figure 3. It is important to note that even the smallest member of this class (**1a**) showed a modest, but relevant, inhibition of both isoforms. A similar behavior was found with 4-chloro-substituted NHI **1d**, whereas the introduction of methyl (**1b**), trifluoromethyl (**1c**), or bromo substituents (**1e**) in position 4

dx.doi.org/10.1021/jm101007q |*J. Med. Chem.* XXXX, XXX, 000–000

caused a drop in the inhibition of LDH-B, whereas the LDH-A inhibition was in some cases increased, as shown by the 32% inhibition of 4-bromo-substituted NHI **1e**. When the bromine atom was shifted to the 6 position, the resulting compound (**1f**) proved to be less active than its 4-substituted counterpart **1e**. Encouraged by these preliminary results obtained with extremely simple modifications of the NHI scaffold, we introduced a phenyl group in the 4, 5, and 6 positions of the central ring. In spite of the poor results obtained with 4-phenyl-substituted derivative **1g**, we were pleased to find a dramatic increase of the LDH-A inhibition level when the phenyl group was present in position 5 (**1h**) or in position 6 (**1i**), with a 99% and a 84% inhibition, respectively. Both compounds showed practically no detectable inhibition of the other isoform (<3%), thus revealing a good level of selectivity. The presence of a 4-CF_3 and a 6-phenyl in compound **1j** caused a notable 87% LDH-A inhibition at 125 μM, although a minimal residual activity on LDH-B (11% at the same concentration) could be detected. The replacement of the 6-phenyl group with a COOH-mimicking heteroaryl portion, such as the tetrazole, caused a dramatic decrease in the inhibitory potency of the resulting compound (**1k**) with a poor 11% inhibition on LDH-A. Methyl ester **4i** gave very modest inhibition of both LDH-A (4%) and LDH-B (8%). *O*-Methylated NHI **8** was completely inactive on both isoforms, whereas indoles **10h,i** proved to be modest nonselective inhibitors of both LDH-A and LDH-B.

These results confirm that when the "*N*-OH/COOH" pharmacophoric motif is modified, the enzyme inhibition potency is negatively affected and that compounds possessing phenyl rings, either at the 5 (**1h**) or at the 6 position (**1i,j**), are the most potent and selective inhibitors of LDH-A. On the basis of this information, these compounds (**1h**−**j**) were selected for a complete enzyme kinetic analysis to verify their type of inhibition versus both the cofactor and the substrate.

We first evaluated the apparent Michaelis−Menten constants (K_m) of NADH and pyruvate for LDH-A, measured from Lineweaver−Burk plots. Then we evaluated the apparent K_m' in the presence of inhibitors **1h**−**j** (concentration range of 25−100 μM). From the values of K_m' so obtained, K_i values for each single inhibitor were determined using double-reciprocal Lineweaver−Burk plots (Figure 4), and their values are reported in Table 1.

Compounds **1h**−**j** were all found to be *competitive* inhibitors of LDH-A with respect to both NADH and pyruvate (Figure 4) in the conversion of pyruvate to lactate catalyzed by this enzyme, whereby NADH is converted to NAD^+. In fact, the V_{max} value proved to be independent from the concentration of the inhibitor, a fact different from the K_m' values, which were instead dependent on concentrations. These compounds were shown to be potent inhibitors of LDH-A with K_i values reaching the low micromolar range (Table 1) with inhibitor **1j** (K_i = 8.9 μM vs NADH and 4.7 μM vs pyruvate). Isoform selectivity was confirmed by the observation that inhibition of the other isoform LDH-B was either negligible (entries 1 and 2) or very low (entry 3).

Molecular Modeling. In order to further understand and characterize the interaction of these compounds with the LDH-A active site, the most promising ligand (**1j**) was analyzed by docking modeling studies into an open loop conformation of the enzyme. The compound was docked into LDH-A using the GOLD program,[41] and the best pose was used as starting geometry for molecular dynamics (MD) calculations. MD simulation for 10 ns with explicit water was carried out. In the first 1.2 ns all the α carbons of the protein were blocked with a harmonic force constant, which decreased during these 1.2 ns from 10 to 1 kcal/(mol·Å^2), while in the last 7.8 ns, no constraints were applied. The system reached an apparent equilibrium after about

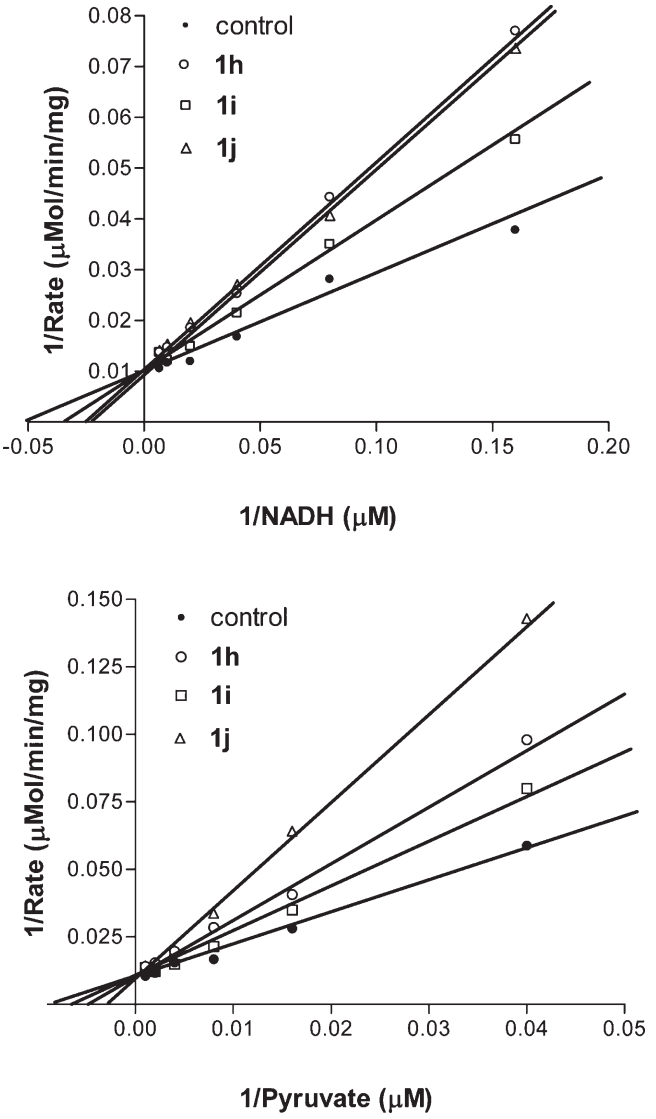

Figure 4. Lineweaver−Burk plots determined from triplicate experiments with inhibitors **1h**−**j** at 25 μM using average activities: competition experiments with NADH (top) and pyruvate (bottom).

Table 1. LDH Inhibition Data (K_i for LDH-A, % Inhibition at 125 μM for LDH-B) Obtained with Compounds 1h−j[a]

		LDH-A (K_i, μM)		LDH-B (% at 125 μM)
entry	compd	[NADH][b]	[pyruvate][c]	[NADH][b]
1	**1h**	10.4 ± 1.5	15.7 ± 1.5	<3%
2	**1i**	19.8 ± 2.2	35.4 ± 3.4	<3%
3	**1j**	8.9 ± 1.3	4.7 ± 0.5	11% ± 3

[a] K_i determination and percent of inhibition were performed in presence of compounds **1h**−**j** as described in the Experimental Section. Values are reported as the mean ± SD of three or more independent experiments. [b] Saturating concentration (2 mM) of sodium pyruvate and competitive increasing concentrations (12.5−150 μM) of NADH. [c] Saturating concentration (200 μM) of NADH and competitive increasing concentrations (25 μM to 1.0 mM) of sodium pyruvate.

dx.doi.org/10.1021/jm101007q |J. Med. Chem. XXXX, XXX, 000–000

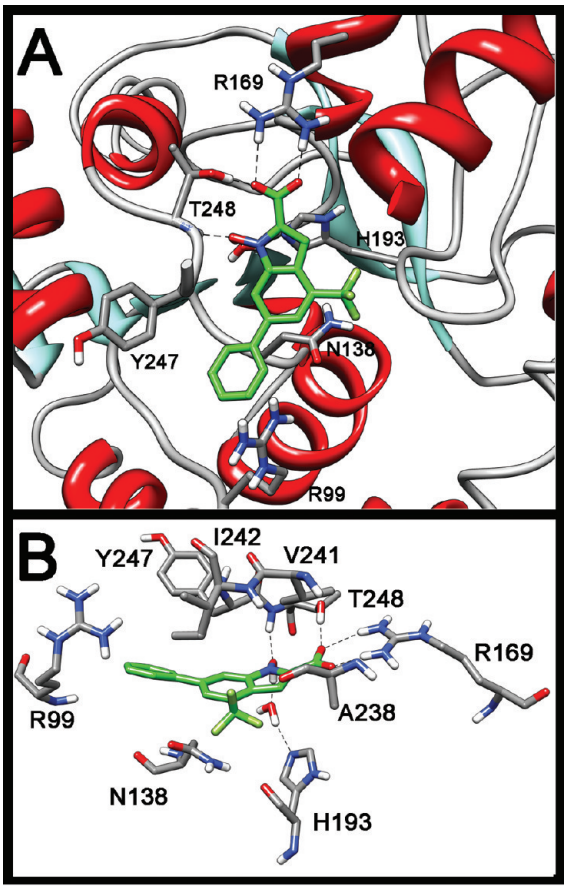

Figure 5. MD simulation results for the complex of LDH with **1j**. Overall disposition of the ligand into LDH (A; residues 240−245 are hidden for a better visualization) and LDH−ligand interactions (B).

0.5 ns of MD, since the total energy for the residual nanoseconds remained constant (Figure S1 in Supporting Information). Analyzing the root-mean-square deviation (rmsd) from the initial model of the α carbons of the proteins, we observed that after an initial increase, the rmsd remained approximately constant around 1.5 Å during the last 5.5 ns (Figure S1 in Supporting Information).

Figure 5 shows the minimized structures of the average of the last 5.5 ns of the MD simulation. In the proposed model the carboxylic group of compound **1j** shows a strong interaction with R169 and T248 (see Figure 5A), whereas the *N*-hydroxy group shows an H-bond interaction with the nitrogen backbone of T248 and a water molecule that mediates the interaction of **1j** with the catalytic H193 (see Figure 5A and Figure 5B). An important role of residues R169, T248, and H193 for the ligand interactions has already been highlighted by the analysis of the X-ray structure of the LDH complexed with the natural substrate pyruvate and NADH (Figure 6). In fact, this structure confirms the interactions between the pyruvate carboxylate group with the arginine and threonine residues of the enzyme, as well as that occurring between the carbonyl oxygen atom of the substrate and the abovementioned histidine amino acid (compare Figures 5 and 6).

The H-bond analysis of the last 5.5 ns of the MD simulation seems to confirm the interactions described above. In particular, as shown in Table S1 (Supporting Information), it is interesting to note that the interaction between the water molecule (bound to H193) and the *N*-hydroxy group is highly conserved during

Figure 6. Representative example of a 1.80 Å resolution X-ray structure of the complex of LDH with NADH (green) and pyruvate (purple): detailed view of the catalytically active site (PDB code: 3D4P).

MD, confirming the important role of this *N*-hydroxy substituent. Furthermore, the analysis of the X-ray structure of *Plasmodium falciparum* isoform of lactate dehydrogenase complexed with 3,7-dihydroxy-2-naphthoic acid[42] revealed the presence of a water molecule able to mediate a H-bond between an OH group of this legend and the catalytic H193 of the enzyme, thus supporting the possible presence of this water molecule also in the human LDH-A form, as we have found with our calculations. As for the 4-(trifluoromethyl)indole central scaffold, it is placed in a cleft mainly delimited by H193, G194, A238, V241, I242, T248. Moreover, N138 is placed in proximity to the trifluoromethyl substituent in our model. According to our calculations, the 6-phenyl group is directed toward the entrance of the binding site cavity and shows lipophilic interactions with I242 and Y247. Overall, this molecular portion seems to partially overlap with the region occupied by the cofactor NADH in the human LDH-A X-ray structure.[31]

Finally, the results obtained by this docking analysis, showing that compound **1j** may occupy the whole substrate pocket and, in part, the cofactor pocket of LDH-A, are in good agreement with the experimental enzyme inhibition data, which indicate that inhibitor **1j** and its analogues **1i,h** are competitive with both pyruvate and NADH.

Cell-Based Reduction of Lactate Production. The ability of inhibitors **1h−j** to reduce the cellular production of lactate was determined by ^{13}C NMR spectroscopy studies on perfused cultures of HeLa cervical cancer cells, incubated with labeled D-[1,6-$^{13}C_2$] glucose. This approach was recently reported as a noninvasive method to detect modifications of the cellular glucose metabolism in real time.[43] D-[1,6-$^{13}C_2$]Glucose undergoes a glycolytic transformation by producing [3-^{13}C]pyruvate, which is then transformed by LDH into [3-^{13}C]lactate (Figure 7A).

In these experiments, cells were treated with 500 μM solutions of inhibitors **1h−j** and the relative production of lactate was measured by integrating the area corresponding to lactate-C3 peak at 20.28 ppm relative to the integration of the glucose-C6 peak at 60.95 ppm (Lac/Glu peak ratio). After addition of D-[1,6-$^{13}C_2$]glucose to the cell culture the Lac/Glu peak area ratio in untreated cells increased over time with a value of 0.16 after 6 h and a higher value of 0.45 after 12 h, thus showing a progressive conversion of glucose to lactate over that period of time (Figure 7B,C). Treatment of cells with a 500 μM solution of compound **1i** (panel D) caused a reduction of that

dx.doi.org/10.1021/jm101007q |*J. Med. Chem.* XXXX, XXX, 000–000

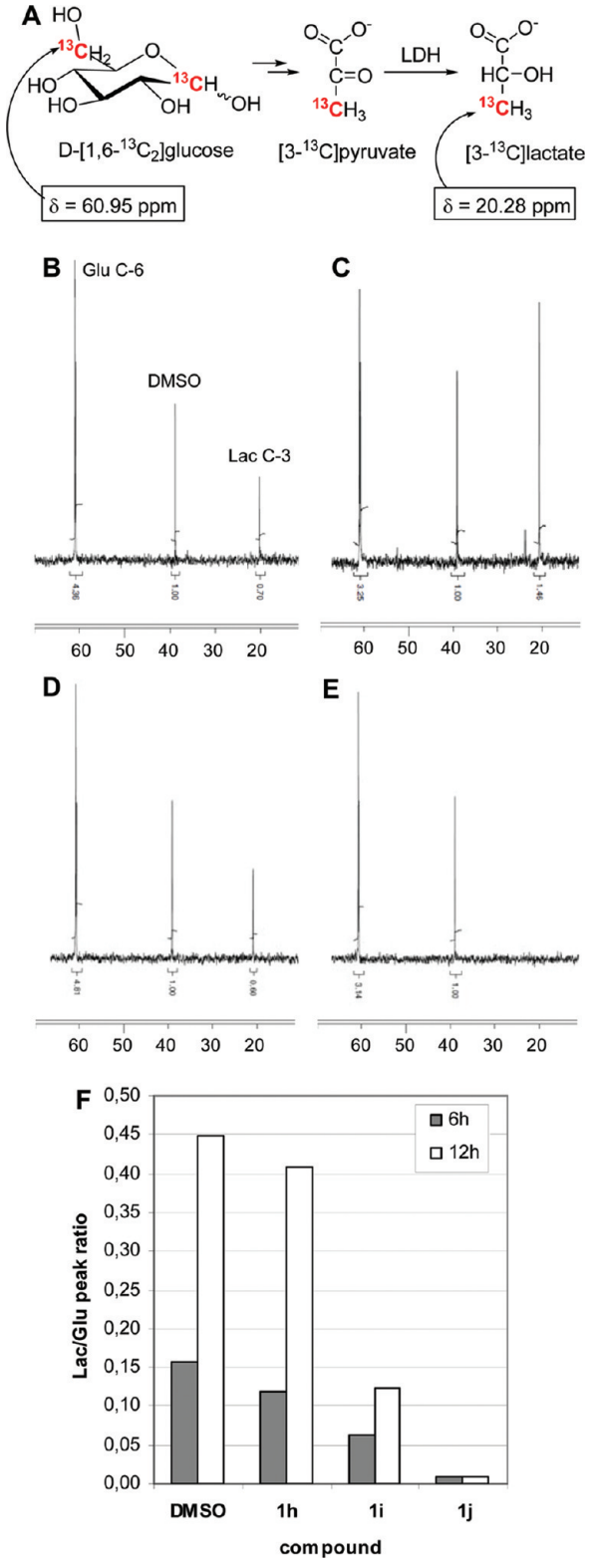

Figure 7. (A) Formation of labeled [3-^{13}C]lactate from D-[1,6-$^{13}C_2$] glucose and relevant ^{13}C NMR peak frequencies. (B–E) ^{13}C NMR spectra of perfused cultures of HeLa cells fed with D-[1,6-$^{13}C_2$]glucose: (B) untreated (DMSO control) after 6 h; (C) untreated (DMSO control) after 12 h; (D) 12 h after addition of **1i** (500 μM); (E) 12 h after addition of **1j** (500 μM). (F) Effect of LDH inhibitors **1h–j** (500 μM) on the production of labeled [3-^{13}C]lactate from D-[1,6-$^{13}C_2$] glucose in HeLa cells.

Table 2. Effects on Cell Growth (IC_{50}, μM) of Different Human Cells by Compounds 1h–j[a]

	IC_{50} (μM)		
cell type	**1h**	**1i**	**1j**
Cancer Cell (ATCC)			
ADDP(ovarian cancer)	14.6 ± 2.8	16.3 ± 3.8	17.0 ± 4.2
A2780/cOHP (ovarian cancer)	13.7 ± 3.6	10.1 ± 2.3	10.8 ± 2.4
H630 (colorectal cancer)	17.7 ± 5.1	15.1 ± 4.9	31.5 ± 7.4
NIH-H2452 (mesothelioma)	45.3 ± 9.7	21.3 ± 4.2	90.2 ± 18.5
NIH-H2052 (mesothelioma)	62.4 ± 11.8	50.5 ± 12.0	73.2 ± 12.4
MSTO-211H (mesothelioma)	2.5 ± 0.5	2.4 ± 0.3	10.6 ± 3.1
NIH-H28 (mesothelioma)	5.8 ± 1.4	7.8 ± 1.9	11.4 ± 3.1
Primary Cancer Culture			
LPC006 (pancreatic cancer)	14.3 ± 2.9	15.7 ± 3.7	16.3 ± 2.5
LPC028 (pancreatic cancer)	48.8 ± 6.5	32.3 ± 7.1	41.2 ± 7.8
LPC067 (pancreatic cancer)	20.9 ± 5.4	18.2 ± 4.7	13.5 ± 3.0
Immortalized Cells			
hTERT-HPNE (ductal pancreatic)	>100	>100	>100
Hs27 (skin fibroblasts)	>100	>100	>100

[a] IC_{50}: inhibitory concentration causing a 50% reduction in cell growth, in μM; values are the mean ± SD from at least two triplicate cytotoxicity sulforhodamine-B (SRB) experiments.

ratio (Lac/Glu peak ratio of 0.12 vs 0.45 for treated and control, respectively) after 12 h, whereas a remarkable drop of lactate production was caused by the same concentration of **1j** (panel E), which showed no detectable amounts of lactate in the ^{13}C NMR spectrum (Lac/Glu peak ratio of <0.01).

The quantitative results obtained with these measurements were plotted in Figure 7F, where the Lac/Glu peak ratios after 6 h (gray bars) and 12 h (white bars) are reported. This graph indicates that compound **1h** displayed only a slight activity under these conditions, in spite of its good activity on the isolated enzyme. This discrepancy may be ascribed to many concurrent factors (permeability through cell membrane, intracellular trafficking, etc.), although no experimental evidence is presently available to support any hypothesis. On the other hand, a significant reduction of lactate production was associated with treatment with **1i**, after 6 and 12 h. Furthermore, compound **1j** proved to be by far the most efficient inhibitor of cellular production of lactate, since in this case no detectable amounts of lactate could be reported at any time interval.

We carried out numerous additional experiments to verify if the Lac/Glu ratio reduction operated by the most active compound **1j** could be detected at concentrations lower than 500 μM, where this ratio was <5% of that obtained in DMSO control experiments (Figure 7). Unfortunately, no reduction of lactate production was observed at concentrations of **1j** less than 400 μM, whereas only a very weak reduction (of 20% compared to control) was detected at 400 μM. These results suggest that there is a "threshold" effect in this experiment that we have executed so that a significant change of the ^{13}C NMR peak ratio of lactate C-3 vs glucose C-6 in the perfused cell medium can only be detected after administration of concentrations as high as 500 μM compound **1j** to the cultured HeLa cells. As a support to the involvement of a specific intervention on LDH-A by **1j**, rather than a nonspecific action on many other possible cellular targets due to the high concentration used, we repeated the same

dx.doi.org/10.1021/jm101007q |J. Med. Chem. XXXX, XXX, 000–000

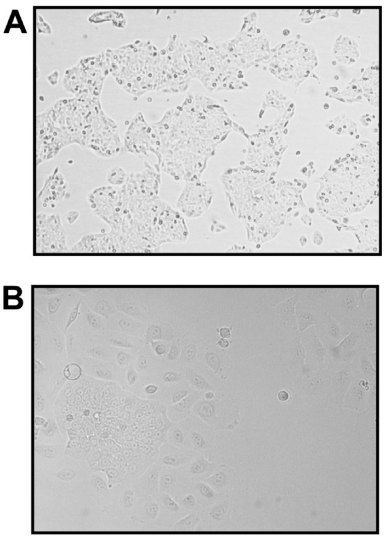

Figure 8. LPC006 primary pancreatic cancer culture in hypoxic conditions: control (A) and treated with **1j** after 48 h of exposure (B). Original magnification is ×10.

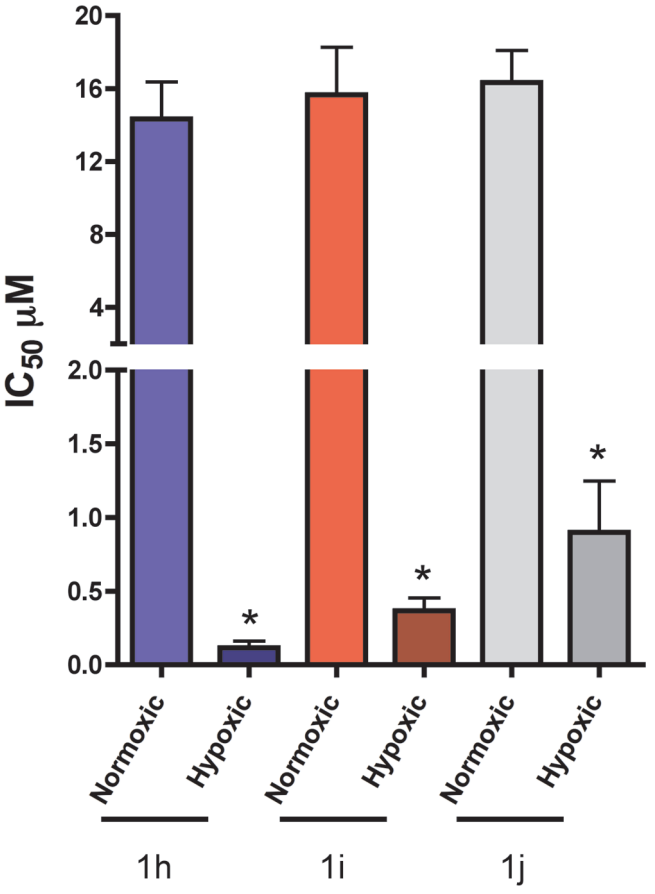

Figure 9. IC_{50} values of compounds **1h**−**j** in LPC006 primary pancreatic cancer culture growing in normoxic and hypoxic conditions: (column) mean values obtained from three independent experiments; (bar), SE; (∗) significantly different from normoxic condition, $P = 0.018$, 0.021, and 0.026 for **1h**, **1i**, and **1j**, respectively.

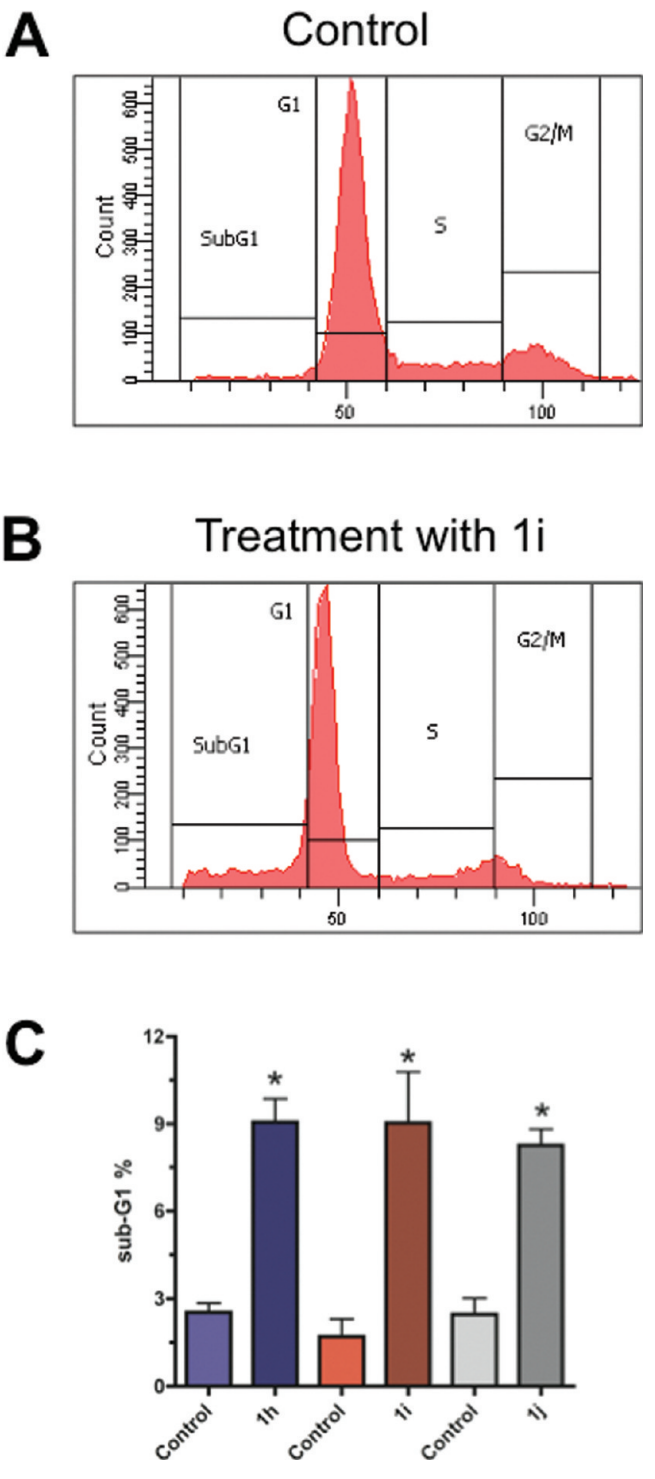

Figure 10. Cell cycle perturbations and apoptosis induction determined by compounds **1h**−**j** in ADDP cells. Representative histograms of cell cycle distribution in untreated (A) and treated (B) cells. (C) Analysis of apoptosis as detected by the appearance of the sub-G1 cell subpopulation: (column) mean values obtained from three independent experiments; (bar) SE; (∗) significantly different ($P < 0.05$) from controls (untreated cells).

experiments with 500 μM solutions of other NHI carboxylates **1b**, **1c**, and **1g**, which are structurally similar to **1j** but do not inhibit LDH-A. Under these conditions, none of the above-mentioned LDH-inactive compounds caused a significant reduction of lactate production. Collectively, these results suggest that in spite of the high concentrations needed, the effect of **1j** on the

dx.doi.org/10.1021/jm101007q |J. Med. Chem. XXXX, XXX, 000–000

cellular transformation of glucose into lactate is due to its inhibitory activity on LDH-A.

In Vitro Effects on Cell Proliferation and Cell Cycle Distribution. The growth inhibitory effect of compounds **1h**−**j** was assayed on a wide range of cells, including cancer cells from different solid tumors, cancer cells resistant to common chemotherapeutic drugs, primary cultures, and normal immortalized cell lines. Exposure of cells to compounds for 48 h resulted in a dose-dependent decrease in cell viability. The compounds were active against all the tumor cells, with IC_{50} values ranging from 2.4 ± 0.3 μM (**1i** in the MSTO-211H cells) to 90.2 ± 18.5 μM (**1j** in the H2452 cells). Fortunately, the compounds were not indiscriminately cytotoxic, as indicated by the observation that the IC_{50} was not reached at 100 μM, the highest concentration tested, in the human pancreatic duct epithelial-like cell line hTERT-HPNE as well as in the skin fibroblasts Hs27 (Table 2). As a negative control, we used compound **1c** which did not give any appreciable inhibition of the cancer cell lines (IC_{50} > 100 μM).

Of note, compounds **1i,j** proved to be superior to cisplatin and oxaliplatin in the ovarian cancer cells with respect to cytotoxicity. Indeed, the IC_{50} values of cisplatin and oxaliplatin in the ADDP and A2780/C-OHP cells were >20 μM.[44] Furthermore, all of the tested compounds were more active than 5-fluorouracil (5-FU) on the inhibition of cell growth in the primary pancreatic cell cultures. In particular, the IC_{50} of 5-FU was 176.3 ± 64.1 μM in the LPC006, 107.1 ± 20.0 μM in the LPC028, and 95.5 ± 24.9 μM in the LPC067 cells, while the IC_{50} values of compounds **1h**−**j** were always below 50 μM in the same cells (Table 2).

To ascertain whether the biological activity of compounds **1h**−**j** could be affected by the hypoxic conditions, these compounds were also tested on LPC006 cells under hypoxic exposure at different concentrations (1−100 μM). These experiments showed a strong increase in the inhibitory effect on cell proliferation (Figure 8B) with respect to untreated cells (Figure 8A). In particular IC_{50} values of compounds **1h**, **1i**, and **1j** were 0.10 ± 0.04, 0.36 ± 0.12, and 0.90 ± 0.48 μM, respectively, thus showing a statistically significant ($P < 0.05$) reduction in IC_{50} values for all the compounds under hypoxic conditions when compared to their activities in normoxygenated cells (Figure 9).

The ability of compounds **1h**−**j** to affect cell cycle distribution and induce cell death by apoptosis was investigated on cells treated for 24 h, using a flow cytometry analysis of DNA content. The exposure of ADDP and H630 cells to compounds **1h**−**j** was indeed able to dose-dependently induce cell cycle disturbance. In particular, at IC_{50} concentration, all the compounds displayed a similar ability to slightly increase the G1 phase and induce apoptosis, with generation of DNA fragments, as detected by the appearance of the sub-G1 cell subpopulation (Figure 10).

CONCLUSIONS

A new class of inhibitors of human LDH-A enzyme was identified in a series of *N*-hydroxy-2-carboxy-substituted indoles. These compounds constitute, to the best of our knowledge, the first example in the scientific literature so far of LDH-A inhibitors that were deliberately designed and synthesized as prospective anticancer agents. These inhibitors showed competitive behavior with NADH and pyruvate and a generally high preference for the A-isoform versus the B-isoform. Their good activities are expressed by the calculated K_i values, reaching the low micromolar range (as low as 4.7 μM for **1j** vs Pyr). Cellular assays confirmed that they can block cancer cell proliferation, especially under hypoxic conditions, and their mechanism of action was supported by the reduction the lactate production in HeLa cells upon exposure to these inhibitors. Overall, these compounds provide a further opportunity to evalutate LDH-A inhibition as an anticancer strategy and add to the growing efforts devoted to targeting glucose metabolism for cancer therapy.

EXPERIMENTAL SECTION

Chemistry. Commercially available chemicals were purchased from Sigma-Aldrich or Alfa Aesar and used without further purification. NMR spectra were obtained with a Varian Gemini 200 MHz spectrometer. Chemical shifts (δ) are reported in parts per million downfield from tetramethylsilane and referenced from solvent references. Electron impact (EI, 70 eV) mass spectra were obtained on a Thermo Quest Finningan (TRACE GCQ plus MARCA) mass spectrometer. Purity was routinely measured by HPLC on a Waters SunFire RP 18 (3.0 mm × 150 mm, 5 μm) column (Waters, Milford, MA, www.waters.com) using a Beckmann SystemGold instrument consisting of a chromatography 125 solvent module and a 166 UV detector. Mobile phases were 10 mM ammonium acetate in Millipore purified water (A) and HPLC grade acetonitrile (B). A gradient was formed from 5% to 80% of B in 10 min and held at 80% for 10 min. Flow rate was 0.7 mL/min, and injection volume was 30 μL. Retention times (HPLC, t_R) are given in minutes. Compound HPLC purity was determined by monitoring at 254 and 300 nm and was found to be in the range 96−99% unless otherwise noted. Chromatographic separations were performed on silica gel columns by flash (Kieselgel 40, 0.040−0.063 mm; Merck) or gravity column (Kieselgel 60, 0.063−0.200 mm; Merck) chromatography. Reactions were followed by thin-layer chromatography (TLC) on Merck aluminum silica gel (60 F_{254}) sheets that were visualized under a UV lamp. Evaporation was performed in vacuo (rotating evaporator). Sodium sulfate was always used as the drying agent. Microwave assisted reactions were run in a CEM or Biotage microwave synthesizer. Yields refer to isolated and purified products. Precursors **2h**[45] and **2i**[46] were previously reported.

4-Methyl-3-nitro-5-(trifluoromethyl)biphenyl (2j). Iodo-aryl derivative **5**[38] (500 mg, 1.51 mmol) was placed in a vial together with phenylboronic acid (203 mg, 1.66 mmol), sodium carbonate (480 mg, 4.53 mmol), $Pd(OAc)_2$ (1.4 mg, 0.006 mmol), tetrabutylammonium bromide (486 mg, 1.51 mmol) and water (3 mL). The vial was sealed and heated under stirring at 150 °C in a microwave reactor for 5 min. The reaction mixture was then diluted with water and repeatedly extracted with EtOAc. The organic phase was dried and evaporated to afford a crude residue that was purified by column chromatography (*n*-hexane/EtOAc 9:1, R_f = 0.48) to give pure **2j** (407 mg, 96% yield); ^{1}H NMR ($CDCl_3$) δ (ppm): 2.60 (q, 2H, J = 1.3 Hz), 7.44−7.62 (m, 5H), 8.07 (d, 1H, J = 1.5 Hz), 8.11 (d, 1H, J = 1.5 Hz). MS m/z 281 (M^+, 58), 264 (M^+ −OH, 100).

General Procedure for the Preparation of Ketoesters 3h,i.[35] Nitrotoluene derivatives **2h,i** (8.5 mmol) and dimethyl oxalate (5.00 g, 42.3 mmol) were dissolved in anhydrous DMF (15 mL), and the resulting solution was added dropwise under nitrogen to a stirred suspension of sodium hydride (60% dispersion in mineral oil, 4.0 equiv) in DMF (20 mL) at 0 °C. The mixture was stirred at room temperature until consumption of starting material (TLC). Then it was diluted with 1 N HCl or saturated aqueous NH_4Cl and extracted with EtOAc. The organic phase was dried and evaporated to afford a crude residue that was purified by column chromatography, using the indicated eluant, to give the desired ketoesters.

Methyl 3-(4-Nitrobiphenyl-3-yl)-2-oxopropanoate (3h). Yield: 77% from **2h**. R_f = 0.34 (*n*-hexane/EtOAc 7:3). ^{1}H NMR ($CDCl_3$) δ (ppm): 3.96 (s, 3H), 4.62 (s, 2H), 7.44−7.67 (m, 6H), 7.70 (dd, 1H, J = 8.6, 2.0 Hz), 8.28 (d, 1H, J = 8.6 Hz). Signals imputable to the enol form (~30%)

dx.doi.org/10.1021/jm101007q |J. Med. Chem. XXXX, XXX, 000–000

δ (ppm): 3.97 (s, 3H), 6.66 (d, 1H, *J* = 1.5 Hz, exchangeable), 7.06 (d, 1H, *J* = 1.3 Hz), 8.04 (d, 1H, *J* = 8.4 Hz), 8.46 (d, 1H, *J* = 2.0 Hz).

Methyl 3-(3-Nitrobiphenyl-4-yl)-2-oxopropanoate (3i). Yield: 81% from **2i**. R_f = 0.25 (*n*-hexane/EtOAc 7:3). ^{1}H NMR ($CDCl_3$) δ (ppm): 3.96 (s, 3H), 4.58 (s, 2H), 7.40 (d, 1H, *J* = 8.1 Hz), 7.44−7.54 (m, 3H), 7.58−7.65 (m, 2H), 7.85 (dd, 1H, *J* = 7.9, 2.0 Hz), 8.40 (d, 1H, *J* = 2.0 Hz). Signals imputable to the enol form (∼20%) δ (ppm): 3.92 (s, 3H), 6.70 (bs, 1H, exchangeable), 6.97 (s, 1H), 7.83 (dd, 1H, *J* = 8.2, 1.9 Hz), 8.13 (d, 1H, *J* = 1.8 Hz), 8.34 (d, 1H, *J* = 8.4 Hz).

Methyl 3-(3-Nitro-5-(trifluoromethyl)biphenyl-4-yl)-2-oxopropanoate (3j). Potassium *tert*-butoxide (135 mg, 1.2 mmol) was dispersed in anhydrous diethyl ether (2.0 mL) at 0 °C under nitrogen, and dry methanol was added (0.2 mL) until complete dissolution was obtained. Next, dimethyl oxalate (142 mg, 1.2 mmol) was added and stirring was continued at 0 °C for 15 min. Finally, a solution of **2j** (281 mg, 1.0 mmol) in dry Et_2O (1.5 mL) was slowly added at the same temperature, and the resulting reddish suspension was then left under stirring at room temperature for 48 h. The mixture was diluted with EtOAc and 1 N aqueous HCl. The organic phase was washed with saturated $NaHCO_3$ and brine, then dried and evaporated to afford a crude residue that was purified by column chromatography (*n*-hexane/EtOAc 9:1, R_f = 0.25) to give pure **3j** (301 mg, 82% yield). ^{1}H NMR ($CDCl_3$) δ (ppm): 3.98 (s, 3H), 4.71 (s, 2H), 7.48−7.65 (m, 5H), 8.19 (d, 1H, *J* = 1.8 Hz), 8.44 (d, 1H, *J* = 1.8 Hz). Signals imputable to the enol form (∼10%) δ (ppm): 3.95 (s, 3H), 6.19 (d, 1H, *J* = 1.6 Hz, exchangeable), 6.80−6.82 (m, 1H). MS *m*/*z* 367 (M^+, 5), 308 ($M^+ - COOCH_3$, 17), 280 ($M^+ - COOCH_3 - CO$, 100).

General Procedure for the Reductive Cyclization Leading to *N*-Hydroxyindoles 4h−j and Indoles 9h,i. Ketoesters **3h−j** (1.0 mmol) were dissolved in anhydrous DME (1.0 mL), and the resulting solution was added dropwise to a cooled (0 °C) solution of $SnCl_2 \cdot 2H_2O$ (2.2 mmol) in DME (1.0 mL) containing activated 4 Å molecular sieves. The reaction mixture was stirred under nitrogen at room temperature until consumption of starting material (TLC). Then it was diluted with water and extracted with EtOAc. The organic phase was dried and evaporated to afford a crude residue that was purified by column chromatography over iron-free silica gel,[47] using the indicated eluant, to give the desired *N*-hydroxyindoles.

Methyl 1-Hydroxy-5-phenyl-1*H*-indole-2-carboxylate (4h). Yield: 21% from **3h**. R_f = 0.27 (*n*-hexane/CH_2Cl_2 2:8). ^{1}H NMR ($CDCl_3$) δ (ppm): 4.01 (s, 3H), 7.08 (s, 1H), 7.33−7.37 (m, 1H), 7.40−7.49 (m, 2H), 7.60−7.66 (m, 4H), 7.82−7.84 (m, 1H), 10.27 (bs, 1H).

Methyl 5-Phenyl-1*H*-indole-2-carboxylate (9h). Yield: 33% from **3h**. R_f = 0.38 (*n*-hexane/CH_2Cl_2 2:8). ^{1}H NMR ($CDCl_3$) δ (ppm): 3.97 (s, 3H), 7.27 (dd, 1H, *J* = 2.0, 1.1 Hz), 7.33−7.37 (m, 1H), 7.41−7.51 (m, 3H), 7.56−7.66 (m, 3H), 7.88−7.90 (m, 1H), 8.90 (bs, 1H).

Methyl 1-Hydroxy-6-phenyl-1*H*-indole-2-carboxylate (4i). Yield: 23% from **3i**. R_f = 0.24 (*n*-hexane/EtOAc 8:2). ^{1}H NMR ($CDCl_3$) δ (ppm): 4.01 (s, 3H), 7.05 (d, 1H, *J* = 0.9 Hz), 7.35−7.51 (m, 4H), 7.67−7.75 (m, 4H), 10.26 (bs, 1H).

Methyl 6-Phenyl-1*H*-indole-2-carboxylate (9i). Yield: 45% from **3i**. R_f = 0.31 (*n*-hexane/EtOAc 8:2). ^{1}H NMR ($CDCl_3$) δ (ppm): 3.96 (s, 3H), 7.27 (dd, 1H, *J* = 2.0, 0.9 Hz), 7.36−7.51 (m, 4H), 7.61−7.68 (m, 3H), 7.75 (d, 1H, *J* = 8.4 Hz), 8.93 (bs, 1H).

Methyl 1-Hydroxy-6-phenyl-4-trifluoromethyl-1*H*-indole-2-carboxylate (4j). Yield: 34% from **3j**. R_f = 0.24 (*n*-hexane/EtOAc 7:3). ^{1}H NMR ($CDCl_3$) δ (ppm): 4.04 (s, 3H), 7.21 (qd, 1H, *J* = 1.6, 1.0 Hz), 7.40−7.54 (m, 3H), 7.66−7.71 (m, 3H), 7.91−7.94 (m, 1H), 10.52 (bs, 1H). ^{13}C NMR (acetone-d_6) δ (ppm): 52.85, 102.34, 111.30, 119.10 (q, *J* = 4.6 Hz), 122.55, 125.08 (q, *J* = 32.8 Hz), 124.44 (q, *J* = 270.4 Hz), 125.14, 127.51 (2C), 128.05, 129.13 (2C), 134.02, 135.30, 138.43, 140.16, 164.27. MS *m*/*z* 335 (M^+, 100), 321 ($M^+ - CH_2$, 90), 319 ($M^+ - O$, 7), 305 ($M^+ - CH_2 - O$, 9), 259 ($M^+ - CH_2 - H_2O - CO_2$, 81), 190 ($M^+ - CH_2 - H_2O - CO_2 - CF_3$, 81). HPLC, t_R = 12.1 min.

Preparation of Final Products 1h−j. General Procedure. Pure methyl esters **4h−j** (0.5 mmol) were dissolved in a 1:1 mixture of THF/methanol (5 mL) and treated with 1.5 mL of 2 N aqueous solution of LiOH. The reaction was monitored by TLC, and after consumption of starting material, the mixture was treated with 1 N aqueous HCl and extracted with EtOAc. The organic phase was dried and evaporated to afford the desired carboxylic acid derivatives.

1-Hydroxy-5-phenyl-1*H*-indole-2-carboxylic Acid (1h). Yield: 90% from **4h**. ^{1}H NMR (DMSO-d_6) δ (ppm): 7.04 (d, 1H, *J* = 0.9 Hz), 7.32−7.36 (m, 1H), 7.42−7.53 (m, 2H), 7.60−7.70 (m, 4H), 7.90 (t, 1H, *J* = 0.9 Hz). ^{13}C NMR (DMSO-d_6) δ (ppm): 104.51, 110.10, 119.85, 119.93, 121.46, 124.10, 126.66 (2C), 127.34, 128.85 (2C), 132.67, 135.00, 140.94, 161.39. MS *m*/*z* 253 (M^+, 100), 237 ($M^+ - O$, 40), 190 ($M^+ - H_2O - CO_2 - H$, 62), 165 ($M^+ - H_2O - CO_2 - C_2H_2$, 12). HPLC, t_R = 9.4 min.

1-Hydroxy-6-phenyl-1*H*-indole-2-carboxylic Acid (1i). Yield: 88% from **4i**. ^{1}H NMR (DMSO-d_6) δ (ppm): 7.03 (s, 1H), 7.36−7.52 (m, 4H), 7.62−7.64 (m, 1H), 7.70−7.75 (m, 3H). ^{13}C NMR (acetone-d_6) δ (ppm): 106.08, 108.19, 121.37, 121.83, 123.63, 127.05, 127.96 (2C), 128.06, 129.68 (2C), 137.49, 139.25, 142.18, 162.05. MS *m*/*z* 253 (M^+, 100), 191 ($M^+ - H_2O - CO_2$, 65), 190 ($M^+ - H_2O - CO_2 - H$, 86), 165 ($M^+ - H_2O - CO_2 - C_2H_2$, 32). HPLC, t_R = 9.2 min.

1-Hydroxy-6-phenyl-4-trifluoromethyl-1*H*-indole-2-carboxylic Acid (1j). Yield: 94% from **4j**. ^{1}H NMR (acetone-d_6) δ (ppm): 7.20 (qd, 1H, *J* = 1.8, 0.7 Hz), 7.43−7.58 (m, 3H), 7.80−7.85 (m, 3H), 8.04−8.06 (m, 1H). ^{13}C NMR (acetone-d_6) δ (ppm): 103.43, 112.32, 117.22, 119.01 (q, *J* = 4.8 Hz), 123.81 (q, *J* = 33.0 Hz), 125.47 (q, *J* = 262.8 Hz), 128.07 (2C), 128.71, 129.89 (2C), 133.64, 137.54, 138.52, 140.71, 161.45. MS *m*/*z* 321 (M^+, 100), 305 ($M^+ - O$, 10), 259 ($M^+ - H_2O - CO_2$, 41), 190 ($M^+ - H_2O - CO_2 - CF_3$, 38). HPLC, t_R = 10.5 min.

Docking Calculations. The X-ray structure of the human muscle L-LDH M chain complexed with NADH and oxamate[31] (PDB code 1I10) was taken from the Protein Data Bank.[48] In order to obtain an open loop conformation form of the protein, the loop structure from A96 to K118 was taken from the open conformation of the rabbit muscle L-LDH M chain (PDB code 3H3F).[49] The structure was directly replaced, since between the two loop sequences there is 100% identity.

The so-obtained structure was placed in a rectangular parallelepiped water box. An explicit solvent model for water, TIP3P, was used, and the complex was solvated with a 8 Å water cap. Chlorine ions were added as counterions to neutralize the system. Two steps of minimization were then carried out. In the first stage, we kept the complex fixed with a position restraint of 500 kcal/(mol·Å^2) and we solely minimized the positions of the water molecules. In the second stage, we minimized the entire system through 5000 steps of steepest descent followed by conjugate gradient (CG) until a convergence of 0.05 kcal/(mol·Å) was attained.

The ligand was built using Maestro, version 9.0,[50] and was minimized using the CG method until a convergence value of 0.05 kcal/(mol·Å) was reached. The minimization was carried out in a water environment model (generalized Born/surface area model) using the MMFFs force field and a distance-dependent dielectric constant of 1.0. Automated docking was carried out by means of the GOLD program, version 4.1.1.[41] The region of interest used by GOLD was defined in order to contain the residues within 10 Å from the original positions of NADH and oxamate in the X-ray structures. The "allow early termination" option was deactivated. The remaining GOLD default parameters were used, and the ligand was submitted to 30 genetic algorithm runs by applying the ChemScore fitness function. The best docked conformation was taken into account.

MD Simulations. All simulations were performed using AMBER, version 10.[51] MD simulations were carried out using the parm03 force field at 300 K. The complex was placed in a rectangular parallelepiped

dx.doi.org/10.1021/jm101007q |*J. Med. Chem.* XXXX, XXX, 000–000

water box. An explicit solvent model for water, TIP3P, was used, and the complex was solvated with a 10 Å water cap. Chlorine ions were added as counterions to neutralize the system. Prior to MD simulations, two steps of minimization were carried out using the same procedure described above. Particle mesh Ewald (PME) electrostatics and periodic boundary conditions were used in the simulation.[52] The MD trajectory was run using the minimized structure as the starting conformation. The time step of the simulations was 2.0 fs with a cutoff of 10 Å for the nonbonded interaction, and SHAKE was employed to keep all bonds involving hydrogen atoms rigid. Constant-volume periodic boundary MD was carried out for 400 ps, during which the temperature was raised from 0 to 300 K. Then 9.6 ns of constant pressure periodic boundary MD was carried out at 300 K using the Langevin thermostat to maintain constant the temperature of our system. In the first 1.2 ns, all the α carbons of the protein were blocked with a harmonic force constant, which decreased during these 1.2 ns from 10 to 1 kcal/(mol·Å^2), while in the last 7.8 ns, no constraints were applied. General Amber force field (GAFF) parameters were assigned to the ligand, while partial charges were calculated using the AM1-BCC method as implemented in the Antechamber suite of AMBER 10. The final structure of the complex was obtained as the average of the last 5.5 ns of MD minimized by the CG method until a convergence of 0.05 kcal/(mol·Å). The average structure was obtained using the ptraj program implemented in AMBER 10.

Enzyme Kinetics Experiments. The oxidation of NADH is observed at 340 nm and in the absence of interfering reactions is a direct measure of the reduction of pyruvate to lactate. The apparent Michaelis−Menten constants (K_m) of LDH-A and LDH-B were measured from Lineweaver−Burk plots. The reaction velocity of purified human LDH-A and LDH-B was determined by a decrease in absorbance at 340 nm of NADH, and the value of optical density was determined at 30 s intervals for 5 min.

LDH-A Inhibition Assay. The effect of compounds **1a**−**k**, **4i**, **8**, **10h**−**i** on LDH-A enzyme activity was measured using purified human lactate dehydrogenase isoform 5 (*h*LDH5, LDH-A_4, Lee Biosolution, Inc.). LDH activity was determined at 37 °C by measuring the oxidation of NADH spectrophotometrically at 340 nm as a function of time. The K_m values of LDH-A for NADH and pyruvate were determined in saturating conditions as described below. In 100 mM sodium phosphate buffer (pH 7.4), 0.005 units of LDH-A were combined with 2 mM sodium pyruvate (pyruvate-saturated) and 12.5−150 μM NADH, or 200 μM NADH (NADH-saturated) and 25 μM to 1 mM sodium pyruvate. These conditions were used for all assays. The reaction velocity of LDH-A was determined spectrophotometrically (Lambda 25, PerkinElmer) by a decrease in absorbance at 340 nm (ε = 6.2 mM^{-1} cm^{-1}) of NADH. Michaelis−Menten constants for substrates were determined from initial rate measurements at 37 °C by nonlinear regression analysis with the GraphPad Prism 3.0. Under these conditions NADH showed a K_m of 20.0 μM and a V_{max} of 62.5 (μmol/min)/mg, whereas pyruvate showed a K_m of 120 μM and a V_{max} of 62.5 (μmol/min)/mg. Compounds **1a**−**k**, **4i**, **8**, **10h**−**i** were dissolved in stock solutions of DMSO (concentrations of DMSO during the initial rate measurements did not exceed 0.5%). Using 25 μM NADH and 2 mM sodium pyruvate, we initially evaluated the percent inhibition of the compounds. We then carried out kinetic studies only on compounds that showed ≥50% inhibition (**1h**−**j**). Then we evaluated the apparent K_m' values in the presence of inhibitors **1h**−**j** (25−100 μM). From the values of K_m' so obtained, K_i values for each single inhibitor were determined using double-reciprocal plots.

LDH-B Inhibition Assay. The effect of compounds **1a**−**k**, **4i**, **8**, **10h**−**i** on LDH-B enzyme activity was measured using purified human lactate dehydrogenase isoform 1 (*h*LDH1, LDH-B_4, ERM AD453/IFCC from Sigma) as described before for LDH-A, only in pyruvate-saturating conditions. Under these conditions NADH showed a K_m of 27 μM and a V_{max} of 65 (μmol/min)/mg. The inhibition percentage of compounds **1a**−**k**, **4i**, **8**, **10h**−**i** was determined as described above.

NMR Experiments on Perfused Cell Cultures. These experiments were conducted as previously reported.[43] Briefly, HeLa cells were grown in 24-well plates in RPMI-1640 medium supplemented with 10% FBS and 1% penicillin/streptomycin at 37 °C in a 5% CO_2, 95% humidity incubator to a confluency of 80%. The medium was aspirated, and the cells were washed by incubating with glucose-free DMEM (10% dialyzed FBS) without phenol red for 15 min. The medium was replaced with 990 μL of DMEM supplemented with 10 mM D-[1,6-$^{13}C_2$]glucose (purchased from Omicron Biochemicals, Inc., South Bend, IN). DMSO stocks of each compound for each concentration were prepared at 100× the final desired concentration and added to the cells (1% DMSO final concentration in wells). Vehicle controls were included in each plate. Plates were incubated under normoxia in a 37 °C, 5% CO_2, 95% humidity incubator. After an incubation time of 6 and 12 h, an amount of 500 μL from each well was collected and the samples were stored at −20 °C. For the preparation of NMR tubes, the samples were defrosted and 100 μL of deuterium oxide was added. The resulting solutions were transferred to 5 mm NMR tubes. ^{13}C spectra were acquired (200 scans) with a 500 MHz Varian spectrometer under fully relaxed conditions with no NOE using a 60° pulse angle and spectral width of 15 000 Hz. Line broadening of 3 Hz was used for the spectra. NMR spectra were analyzed by using MestReC software.

Cell Culture and Cytotoxicity in Normoxic and Hypoxic Exposure. Cell culture medium was from Gibco (Gaithersburg, MD). All other chemicals were from Sigma (St. Louis, MO). Compounds **1h**−**j** were dissolved in sterile dimethylsulfoxide (DMSO) at 10 mM and stored at −20 °C. They were diluted in sterile culture medium immediately before their use.

Human tumor cells H630 (colon cancer), NIH-H2452, NIH-H2052, MSTO-211H, and NIH-H28 (mesothelioma), ADDP and A2780/C-OHP (ovarian cancer, resistant to cisplatin and oxalilplatin, respectively,[44] and human pancreatic duct epithelial-like cell line hTERT-HPNE and skin fibroblasts Hs27 were obtained from the American Type Culture Collection (ATCC, Manassas, VA). Three primary pancreatic cancer cultures (LPC006, LPC028, LPC067) were isolated from patients at the University Hospital of Pisa (Pisa, Italy), as described previously.[53]

Cells were maintained in RPMI 1640 medium supplemented with fetal calf serum (10%), glutamine (2 mM), penicillin (50 IU/mL), and streptomicin (50 μg/mL) in an atmosphere of 5% CO_2 and 95% air at 37 °C.

Chemosensitivity tests were performed using the SRB assay as described in the NCI protocol, with slight modifications.[54] Each compound was tested in triplicate at different concentrations (1−100 μM). Control cells were exposed to an equivalent concentration of DMSO (0.25% v/v, negative control). The drug treatment was started on day 1 after plating. Drug incubation time was 48 h. Then cells were precipitated with 25 μL of ice-cold 50% (w/v) trichloroacetic acid and fixed for 60 min at 4 °C. After the SRB, the optical density (OD) of each well was measured at 492 nm, using a plate reader for absorbance. Values were corrected for background OD using wells only containing medium. The percentage of growth (PG) was calculated with respect to untreated control cells (C) at each of the drug concentration levels based on the difference in OD at the start (T_0) and end of drug exposure (T). Therefore, if $T \geq T_0$, the calculation is $100 \times [(T - T_0)/(C - T_0)]$. If $T < T_0$, denoting cell killing, the calculation is $100 \times [(T - T_0)/(T_0)]$. The effect is defined as the percentage of cell growth, where 50% growth inhibition concentration (IC_{50}), total growth inhibition (TGI), and 50% cell killing (LC_{50}) represent the concentration at which PG is +50, 0, and −50, respectively. With these calculations a PG value of 0 corresponds to the amount of cells present at the start of drug exposure, while negative PG values denote net cell kill.

All these experiments were also performed in cells under hypoxia conditions, using the incubator IncuSafe (Labo Equipment Sanyo, U.K.). Hypoxic cells were maintained in a controlled atmosphere chamber with a gas mixture containing 1% O_2, 5% (v/v) CO_2, and 94% (v/v) N_2 at 37 °C for 48 h.

dx.doi.org/10.1021/jm101007q |J. Med. Chem. XXXX, XXX, 000–000

Cell Cycle Analysis. Cells were seeded in six-well plates at a density of 2×10^5 cells/well. The drug treatment was started on day 1 after plating, at IC_{50} concentration levels in normoxic conditions, and cells were exposed for 24 h. Then cells were trypsinized, harvested, transferred to test tubes, and centrifuged at 1200 rpm for 10 min. The supernatant was discarded, and the cell pellets were suspended in 500 μL of cold propidium iodide buffer and incubated on ice for 30 min. Flow cytometry determination of DNA content (10 000 cells/sample) was performed using a FACSCalibur flow cytometer (Becton Dickinson, San José, CA, U.S.). The fractions of the cells in G0/G1, S, and G2/M phases were analyzed using the cell cycle analysis software FACS-DIVA, version 6.0 (Becton Dickinson).

Statistical Analysis. All experiments were performed in triplicate and repeated at least twice. Data were expressed as mean values ± SE and analyzed by Student's *t*-test or ANOVA followed by Tukey's multiple comparison test. The level of significance was $P < 0.05$.

■ ASSOCIATED CONTENT

Supporting Information. Detailed synthetic procedures and characterization data of all nonkey compounds, Figure S1 showing an analysis of the MD simulation of the LDH−**1j** complex, and Table S1 reporting a H-bond analysis of the LDH−**1j** interactions during the last 5.5 ns of MD simulation. This material is available free of charge via the Internet at http://pubs.acs.org.

■ AUTHOR INFORMATION

Corresponding Author
*Telephone: +39 050 2219557. Fax: +39 050 2219605. E-mail: filippo.minutolo@farm.unipi.it.

■ ACKNOWLEDGMENT

Financial support from the European Community (7th Framework Programme, "Marie Curie Actions") through a research grant to F.M. ("Project Coordinator") and to S.R. ("Postdoctoral Fellow") is gratefully acknowledged (Grant "NOXYCANCER-STARV" FP7-PEOPLE-IIF-2008-235016). We thank the support of the European Organization for Research and Treatment of Cancer (EORTC) (Pharmacology and Molecular Mechanisms (PAMM) group) for a minigrant to support initial chemistry and pharmacology studies (to F.M. and G.J.P.). C.G. is grateful to the Italian Ministry for University and Research (MIUR), Rome, Italy, for a Ph.D. fellowship ("Grandi Progetti Strategici"). Dr. Giorgio Placanica and Dr. Caterina Orlando are gratefully acknowledged for technical assistance in the analysis of the chemical products. We thank the School of Chemical Sciences NMR Laboratory of the University of Illinois at Urbana—Champaign for guidance with the ^{13}C NMR experiments monitoring glucose to lactate conversion.

■ ABBREVIATIONS USED

LDH, lactate dehydrogenase; NADH, reduced nicotinamide adenine dinucleotide; HK, hexokinase; 2-DG, 2-deoxyglucose; DCA, dichloroacetate; PDK, pyruvate dehydrogenase kinase; PDH, pyruvate dehydrogenase; PK, pyruvate kinase; HIF, hypoxia inducible factor; GLUT1, glucose transporter 1; OXM, oxamate; HICA, 3-hydroxyisoxazole-4-carboxylic acid; HTCA, 4-hydroxy-1,2,5-thiadiazole-3-carboxylic acid; NHI, *N*-hydroxyindole; MD, molecular dynamics; SRB, sulforhodamine B; 5-FU, 5-fluorouracil; TLC, thin-layer chromatography

■ REFERENCES

(1) Warburg, O. On the origin of cancer cells. *Science* **1956**, *123*, 309–314.

(2) Gatenby, R. A.; Gillies, R. J. Why do cancers have high aerobic glycolysis? *Nat Rev. Cancer* **2004**, *4*, 891–899.

(3) Vander Heiden, M. G.; Cantley, L. C.; Thompson, C. B. Understanding the Warburg effect: the metabolic requirements of cell proliferation. *Science* **2009**, *324*, 1029–1033.

(4) Heddleston, J. M.; Li, Z.; Lathia, J. D.; Bao, S.; Hjelmeland, A. B.; Rich, J. N. Hypoxia inducible factors in cancer stem cells. *Br. J. Cancer* **2010**, *102*, 789–795.

(5) Kroemer, G.; Pouyssegur, J. Tumor cell metabolism: cancer's Achille's heel. *Cancer Cell* **2008**, *13*, 472–482.

(6) (a) Scatena, R.; Bottoni, P.; Pontoglio, A.; Mastrototaro, L.; Giardina, B. Glycolytic enzyme inhibitors in cancer treatment. *Expert Opin. Invest. Drugs* **2008**, *17*, 1533–1545. (b) Sheng, H.; Niu, B.; Sun, H. Metabolic targeting of cancers: from molecular mechanisms to therapeutic strategies. *Curr. Med. Chem.* **2009**, *16*, 1561–1587. (c) Sattler, U. G. A.; Hirschhaeuser, F.; Mueller-Klieser, W. F. Manipulation of glycolysis in malignant tumors: fantasy or therapy? *Curr Med. Chem.* **2010**, *17*, 96–108.

(7) Tennant, D. A.; Durán, R. V.; Gottlieb, E. Targeting metabolic transformation for cancer therapy. *Nat. Rev. Cancer* **2010**, *10*, 267–277.

(8) Price, G. S.; Page, R. L.; Riviere, J. E.; Cline, J. M.; Thrall, D. E. Pharmacokinetics and toxicity of oral and intravenous lonidamine in dogs. *Cancer Chemother. Pharmacol.* **1996**, *38*, 129–135.

(9) Maher, J. C.; Wangpaichitr, M.; Savaraj, N.; Kurtoglu, M.; Lampidis, T. J. Hypoxia-inducible factor-1 confers resistance to the glycolytic inhibitor 2-deoxy-D-glucose. *Mol. Cancer Ther.* **2007**, *6*, 732–741.

(10) Ko, Y. H.; Smith, B. L.; Wang, Y.; Pomper, M. G.; Rini, D. A.; Torbenson, M. S.; Hullihen, J.; Pedersen, P. L. Advanced cancers: eradication in all cases using 3-bromopyruvate therapy to deplete ATP. *Biochem. Biophys. Res. Commun.* **2004**, *324*, 269–275.

(11) Bonnet, S.; Archer, S. L.; Allalunis-Turner, J.; Haromy, A.; Beaulieu, C.; Thompson, R.; Lee, C. T.; Lopaschuk, G. D.; Puttagunta, L.; Bonnet, S.; Harry, G.; Hashimoto, K.; Porter, C. J.; Andrade, M. A.; Thebaud, B.; Michelakis, E. D. A mitochondria-K^+ channel axis is suppressed in cancer and its normalization promotes apoptosis and inhibits cancer growth. *Cancer Cell* **2007**, *11*, 37–51.

(12) Wigfield, S. M.; Winter, S. C.; Giatromanolaki, A.; Taylor, J.; Koukourakis, M. L.; Harris, A. L. PDK-1 regulates lactate production in hypoxia and is associated with poor prognosis in head and neck squamous cancer. *Br. J. Cancer* **2008**, *98*, 1975–1984.

(13) Briasoulis, E.; Pavlidis, N.; Terret, C.; Bauer, J.; Fiedler, W.; Schöffski, P.; Raoul, J.-L.; Hess, D.; Selvais, R.; Lacombe, D.; Bachmann, P.; Fumoleau, P. Glufosfamide administered using a 1-hour infusion given as first-line treatment for advanced pancreatic cancer. A phase II trial of the EORTC-new drug development group. *Eur. J. Cancer* **2003**, *39*, 2334–2340.

(14) Christofk, H. R.; Vander Heiden, M. G.; Harris, M. H.; Ramanathan, A.; Gerszten, R. E.; Wei, R.; Fleming, M. D.; Schreiber, S. L.; Cantley, L. C. The M2 splice isoform of pyruvate kinase is important for cancer metabolism and tumour growth. *Nature* **2008**, *452*, 230–233.

(15) (a) Spoden, G. A.; Mazurek, S.; Morandell, D.; Bacher, N.; Ausserlechner, M. J.; Jansen-Dürr, P.; Eigenbrodt, E.; Zwerschke, W. Isotype-specific inhibitors of the glycolytic key regulator pyruvate kinase subtype M2 moderately decelerate tumor cell proliferation. *Int. J. Cancer* **2008**, *123*, 312–321. (b) Cantley, L. C. Vander Heiden, M. G. Christofk, H. R. Inhibitors of Pyruvate Kinase and Methods of Treating Disease. WO2008019139, 2008.

(16) Christofk, H. R.; Vander Heiden, M. G.; Wu, N.; Asara, J. M.; Cantley, L. C. Pyruvate kinase M2 is a phosphotyrosinebinding protein. *Nature* **2008**, *452*, 181–186.

(17) Boxer, M. B.; Jiang, J. K.; Vander Heiden, M. G.; Shen, M.; Skoumbourdis, A. P.; Southall, N.; Veith, H.; Leister, W.; Austin, C. P.;

Park, H. W.; Inglese, J.; Cantley, L. C.; Auld, D. S.; Thomas, C. J. Evaluation of substituted *N,N′*-diarylsulfonamides as activators of the tumor cell specific M2 isoform of pyruvate kinase. *J. Med. Chem.* **2010**, *53*, 1048–1055.

(18) (a) Koukorakis, M. I.; Giatromanolaki, A.; Simopoulos, C.; Polychronidis, A.; Sivridis, E. Lactate dehydrogenase 5 (LDH5) relates to up-regulated hypoxia inducible factor pathway and metastasis in colorectal cancer. *Clin. Exp. Metastasis* **2005**, *22*, 25–30. (b) Koukorakis, M. I.; Pitiakoudis, M.; Giatromanolaki, A.; Tsarouha, A.; Polychronidis, A.; Sivridis, E.; Simopoulos, C. Oxygen and glucose consumption in gastrointestinal adenocarcinomas: correlation with markers of hypoxia, acidity and anaerobic glycolysis. *Cancer Sci.* **2006**, *97*, 1056–1060. (c) Kolev, Y.; Uetake, H.; Takagi, Y.; Sugihara, K. Lactate dehydrogenase-5 (LDH-5) expression in human gastric cancer: association with hypoxia-inducible factor (HIF-1α) pathway, angiogenic factors production and poor prognosis. *Ann. Surg. Oncol.* **2008**, *15*, 2336–2344.

(19) Koukourakis, M. I.; Giatromanolaki, A.; Sivridis, E.; Bougioukas, G.; Didilis, V.; Gatter, K. C.; Harris, A. L. Lactate dehydrogenase-5 (LDH-5) overexpression in non-small-cell lung cancer tissues is linked to tumour hypoxia, angiogenic factor production and poor prognosis. *Br. J. Cancer* **2003**, *89*, 877–885.

(20) (a) Sørensen, B. S.; Hao, J.; Overgaard, J.; Vorum, H.; Honoré, B.; Alsner, J.; Horsman, M. R. Influence of oxygen concentration and pH on expression of hypoxia induced genes. *Radiother. Oncol.* **2005**, *76*, 187–193. (b) Sørensen, B. S.; Alsner, J.; Overgaard, J.; Horsman, M. R. Hypoxia induced expression of endogenous markers in vitro is highly influenced by pH. *Radiother. Oncol.* **2007**, *83*, 362–366.

(21) (a) Lardner, A. The effects of extracellular pH on immune function. *J. Leukocyte Biol.* **2001**, *69*, 522–530. (b) Fischer, K.; Hoffmann, P.; Voelkl, S.; Meidenbauer, N.; Ammer, J.; Edinger, M.; Gottfried, E.; Schwarz, S.; Rothe, G.; Hoves, S.; Renner, K.; Timischl, B.; Mackensen, A.; Kunz-Schughart, L.; Andreesen, R.; Krause, S. W.; Kreutz, M. Inhibitory effect of tumor cell-derived lactic acid on human T cells. *Blood* **2007**, *109*, 3812–3819.

(22) Fantin, V. R.; St-Pierre, J.; Leder, P. Attenuation of LDH-A expression uncovers a link between glycolysis, mitochondrial physiology, and tumor maintenance. *Cancer Cell* **2006**, *9*, 425–434.

(23) Zhou, M.; Zhao, Y.; Ding, Y.; Liu, H.; Liu, Z.; Fodstad, O.; Riker, A. I.; Kamarajugadda, S.; Lu, J.; Owen, L. B.; Ledoux, S. P.; Tan, M. Warburg effect in chemosensitivity: targeting lactate dehydrogenase-A re-sensitizes Taxol-resistant cancer cells to Taxol. *Mol. Cancer* **2010**, *9*, 33.

(24) Kanno, T.; Sudo, K.; Maekawa, M.; Nishimura, Y.; Ukita, M.; Fukutake, K. Lactate dehydrogenase M-subunit deficiency: a new type of hereditary exertional myopathy. *Clin. Chim. Acta* **1988**, *173*, 89–98.

(25) Granchi, C.; Bertini, S.; Macchia, M.; Minutolo, F. Inhibitors of lactate dehydrogenase isoforms and their therapeutic potentials. *Curr. Med. Chem.* **2010**, *17*, 672–697.

(26) Thornburg, J. M.; Nelson, K. K.; Clem, B. F.; Lane, A. N.; Arumugam, S.; Simmons, A.; Eaton, J. W.; Telang, S.; Chesney, J. Targeting aspartate aminotransferase in breast cancer. *Breast Cancer Res.* **2008**, *10*, R84.

(27) Vander Jagt, D. L.; Deck, L. M.; Royer, R. E. Gossypol: prototype of inhibitors targeted to dinucleotide folds. *Curr. Med. Chem* **2000**, *7*, 479–498.

(28) Cameron, A.; Read, J.; Tranter, R.; Winter, V. J.; Sessions, R. B.; Brady, R. L.; Vivas, L.; Easton, A.; Kendrick, H.; Croft, S. L.; Barros, D.; Lavandera, J. L.; Martin, J. J.; Risco, F.; García-Ochoa, S.; Gamo, F. J.; Sanz, L.; Leon, L.; Ruiz, J. R.; Gabarró, R.; Mallo, A.; Gómez de las Heras, F. Identification and activity of a series of azole-based compounds with lactate dehydrogenase-directed anti-malarial activity. *J. Biol. Chem.* **2004**, *279*, 31429–31439.

(29) Deck, L. M.; Royer, R. E.; Chamblee, B. B.; Hernandez, V. M.; Malone, R. R.; Torres, J. E.; Hunsaker, L. A.; Piper, R. C.; Makler, M. T.; Vander Jagt, D. L. Selective inhibitors of human lactate dehydrogenases and lactate dehydrogenase from the malarial parasite *Plasmodium falciparum*. *J. Med. Chem.* **1998**, *41*, 3879–3887.

(30) Le, A.; Cooper, C. R.; Gouw, A. M.; Dinavahi, R.; Maitra, A.; Deck, L. M.; Royer, R. E.; Vander Jagt, D. L.; Semenza, G. L.; Dang, C. V. Inhibition of lactate dehydrogenase A induces oxidative stress and inhibits tumor progression. *Proc. Natl. Acad. Sci. U.S.A.* **2010**, *107*, 2037–2042.

(31) Read, J. A.; Winter, V. J.; Eszes, C. M.; Sessions, R. B.; Brady, R. L. Structural basis for altered activity of M- and H-isozyme forms of human lactate dehydrogenase. *Proteins* **2001**, *43*, 175–185.

(32) Somei, M. 1-Hydroxyindoles. *Heterocycles* **1999**, *50*, 1157–1211.

(33) Bagley, M. C.; Dale, J. W.; Merritt, E. A.; Xiong, X. Thiopeptide antibiotics. *Chem. Rev.* **2005**, *105*, 685–714.

(34) Somei, M. Recent advances in the chemistry of 1-hydroxyindoles, 1-hydroxytryptophans, and 1-hydroxytryptamines. *Adv. Heterocycl. Chem.* **2002**, *82*, 101–155.

(35) Nicolaou, K. C.; Estrada, A. A.; Freestone, G. C.; Lee, S. H.; Alvarez-Mico, X. New synthetic technology for the construction of *N*-hydroxyindoles and synthesis of nocathiacin I model systems. *Tetrahedron* **2007**, *63*, 6088–6114.

(36) Bykov, E. E.; Lavrenov, S. N.; Preobrazhenskaya, M. N. Quantum-chemical investigation of the dependence of pK_a on the calculated energy of proton removal for certain derivatives of indole and phenol. *Chem. Heterocycl. Compd.* **2006**, *42*, 42–44.

(37) Entwistle, I. D.; Gilkerson, T.; Johnstone, R. A. W.; Telford, R. P. Rapid catalytic transfer reduction of aromatic nitro compounds to hydroxylamines. *Tetrahedron* **1978**, *34*, 213–215.

(38) Hume, W. E.; Tokunaga, T.; Nagata, R. A concise and regioselective synthesis of 6-iodo-4-trifluoromethylisatin, an intermediate in the synthesis of the novel, non-peptidyl growth hormone secretagogue SM-130686. *Tetrahedron* **2002**, *58*, 3605–3611.

(39) Leadbeater, N. E.; Marco, M. Ligand-free palladium catalysis of the Suzuki reaction in water using microwave heating. *Org. Lett.* **2002**, *4*, 2973–2976.

(40) Demko, Z. P.; Sharpless, K. B. Preparation of 5-substituted 1*H*-tetrazoles from nitriles in water. *J. Org. Chem.* **2001**, *66*, 7945–7950.

(41) Verdonk, M. L.; Cole, J. C.; Hartshorn, M. J.; Murray, C. W.; Taylor, R. D. Improved protein−ligand docking using GOLD. *Proteins* **2003**, *52*, 609–623.

(42) Conners, R.; Schambach, F.; Read, J.; Cameron, A.; Sessions, R. B.; Vivas, L.; Easton, A.; Croft, S. L.; Brady, R. L. Mapping the binding site for gossypol-like inhibitors of *Plasmodium falciparum* lactate dehydrogenase. *Mol. Biochem. Parasitol.* **2005**, *142*, 137–148.

(43) DeBerardinis, R. J.; Mancuso, A.; Daikhin, E.; Nissim, I.; Yudkoff, M.; Wehrli, S.; Thompson, C. B. Beyond aerobic glycolysis: transformed cells can engage in glutamine metabolism that exceeds the requirement for protein and nucleotide synthesis. *Proc. Natl. Acad. Sci. U.S.A.* **2007**, *104*, 19345–19350.

(44) Noordhuis, P.; Laan, A. C.; van de Born, K.; Losekoot, N.; Kathmann, I.; Peters, G. J. Oxaliplatin activity in selected and unselected human ovarian and colorectal cancer cell lines. *Biochem. Pharmacol.* **2008**, *76*, 53–61.

(45) Grieve, W. S. M.; Hey, D. H. Substitution in compounds containing two or more phenyl groups. II. The nitration of 3-methylbiphenyl. *J. Chem. Soc.* **1932**, 2245–2247.

(46) Suryadevara, P. K.; Olepu, S.; Lockman, J. W.; Ohkanda, J.; Karimi, M.; Verlinde, C. L. M. J.; Kraus, J. M.; Schoepe, J.; Van Voorhis, W. C.; Hamilton, A. D.; Buckner, F. S.; Gelb, M. H. Structurally simple inhibitors of lanosterol 14α-demethylase are efficacious in a rodent model of acute chagas disease. *J. Med. Chem.* **2009**, *52*, 3703–3715.

(47) Cesario, C.; Miller, M. J. Pd(0)/InI-mediated allylic additions to 4-acetoxy-2-azetidinone: new route to highly functionalized carbocyclic scaffolds. *Org. Lett.* **2009**, *11*, 1293–1295.

(48) Berman, H. M.; Westbrook, J.; Feng, Z.; Gilliland, G.; Bhat, T. N.; Weissig, H.; Shindyalov, I. N.; Bourne, P. E. The Protein Data Bank. *Nucleic Acids Res.* **2000**, *28*, 235–242.

(49) Swiderek, K.; Panczakiewicz, A.; Bujacz, A.; Bujacz, G.; Paneth, P. Modeling of isotope effects on binding oxamate to lactic dehydrogenase. *J. Phys. Chem. B* **2009**, *113*, 12782–12789.

(50) *Maestro*, version 9.0; Schrödinger Inc: Portland, OR, 2009.

(51) Case, D. A.; Darden, T. A.; Cheatham, T. E., III; Simmerling, C. L.; Wang, J.; Duke, R. E.; Luo, R.; Crowley, M.; Walker, R. C.; Zhang, W.; Merz, K. M.; Wang, B.; Hayik, S.; Roitberg, A.; Seabra, G.; Kolossváry, I.; Wong, K. F.; Paesani, F.; Vanicek, J.; Wu, X.; Brozell, S. R.; Steinbrecher, T.; Gohlke, H.; Yang, L.; Tan, C.; Mongan, J.; Hornak, V.; Cui, G.; Mathews, D. H.; Seetin, M. G.; Sagui, C.; Babin, V.; Kollman, P. A. *AMBER*, version 10; University of California: San Francisco, CA, 2008.

(52) York, D. M.; Darden, T. A.; Pedersen, L. G. The effect of long-range electrostatic interactions in simulations of macromolecular crystals: a comparison of the Ewald and truncated list methods. *J. Chem. Phys.* **1993**, *99*, 8345–8348.

(53) Funel, N.; Giovannetti, E.; Del Chiaro, M.; Mey, V.; Pollina, L. E.; Nannizzi, S.; Boggi, U.; Ricciardi, S.; Del Tacca, M.; Bevilacqua, G.; Mosca, F.; Danesi, R.; Campani, D. Laser microdissection and primary cell cultures improve pharmacogenetic analysis in pancreatic adenocarcinoma. *Lab. Invest.* **2008**, *88*, 773–784.

(54) León, L. G.; Carballo, R. M.; Vega-Hernández, M.-C.; Miranda, P. O.; Martín, V. S.; Padrón, J. I.; Padrón, J. M. β'-Hydroxy-α,β-unsaturated ketones: a new pharmacophore for the design of anticancer drugs. Part 2. *ChemMedChem* **2008**, *3*, 1740–1747.